Published August 1, 2011

The myosin-related motor protein Myo2 is an essential mediator of bud-directed mitochondrial movement in yeast

Johannes Förtsch,[1] Eric Hummel,[1] Melanie Krist,[1] and Benedikt Westermann[1,2]

[1]Institut für Zellbiologie and [2]Bayreuther Zentrum für Molekulare Biowissenschaften, Universität Bayreuth, 95440 Bayreuth, Germany

The inheritance of mitochondria in yeast depends on bud-directed transport along actin filaments. It is a matter of debate whether anterograde mitochondrial movement is mediated by the myosin-related motor protein Myo2 or by motor-independent mechanisms. We show that mutations in the Myo2 cargo binding domain impair entry of mitochondria into the bud and are synthetically lethal with deletion of the *YPT11* gene encoding a rab-type guanosine triphosphatase. Mitochondrial distribution defects and synthetic lethality were rescued by a mitochondria-specific Myo2 variant that carries a mitochondrial outer membrane anchor. Furthermore, immunoelectron microscopy revealed Myo2 on isolated mitochondria. Thus, Myo2 is an essential and direct mediator of bud-directed mitochondrial movement in yeast. Accumulating genetic evidence suggests that maintenance of mitochondrial morphology, Ypt11, and retention of mitochondria in the bud contribute to Myo2-dependent inheritance of mitochondria.

Introduction

Mitochondria cannot be made de novo and thus must be inherited upon cell division (Warren and Wickner, 1996; Yaffe, 1999). Mitochondrial inheritance involves growth and division of existing organelles, replication of the mitochondrial genome, and partitioning of the organelles to the daughter cells before cytokinesis. Cytoskeleton-dependent transport plays an important role in the partitioning of mitochondria during cell division and controls their morphology and intracellular distribution (Boldogh and Pon, 2007; Frederick and Shaw, 2007).

Budding yeast *Saccharomyces cerevisiae* has been used extensively to study the molecular mechanisms of organelle inheritance (Catlett and Weisman, 2000; Bretscher, 2003; Pruyne et al., 2004; Fagarasanu and Rachubinski, 2007; Merz et al., 2007). During mitotic growth, yeast cells multiply by asymmetric cell division, a process termed budding. Correct organelle partitioning is achieved by active and directed transport of organelles to the growing bud concomitant with retention of a portion of the organelles in the mother cell. Actin cables that consist of bundles of actin filaments provide the tracks for directed transport processes during cell growth (Pruyne et al., 2004).

Class V myosins are processive molecular motors that transport their cargo toward the plus ends of actin filaments. They are involved in numerous membrane trafficking events (Reck-Peterson et al., 2000; Trybus, 2008). *S. cerevisiae* has two class V myosins, Myo2, which is encoded by an essential gene, and Myo4, which is encoded by a nonessential gene. While Myo4 mediates the transport of mRNAs and movement of ER tubules, Myo2 plays a major role in the transport of secretory vesicles and segregation of membrane-bounded organelles including vacuoles, peroxisomes, and organelles of the secretory pathway (Matsui, 2003; Pruyne et al., 2004; Weisman, 2006; Fagarasanu et al., 2010).

Several lines of evidence suggest that Myo2 is involved in mitochondrial transport. Several conditional *myo2* mutants show defects in mitochondrial distribution toward the bud (Itoh et al., 2002, 2004; Boldogh et al., 2004; Altmann et al., 2008), and cells depleted of Myo2 or its essential light chain, Mlc1, contain abnormal mitochondria that are devoid of mitochondrial DNA (Altmann and Westermann, 2005; Altmann et al., 2008). Moreover, isolated mitochondria lacking functional Myo2 lose

Correspondence to Benedikt Westermann: benedikt.westermann@uni-bayreuth.de

Abbreviations used in this paper: 5-FOA, 5-fluoroorotic acid; DIC, differential interference contrast; ERMES, ER-mitochondria encounter structure; mt, mitochondria targeted; WT, wild type.

Supplemental Material can be found at:
http://jcb.rupress.org/content/suppl/2011/07/29/jcb.201012088.DC1.html

The Rockefeller University Press $30.00
J. Cell Biol. Vol. 194 No. 3 473–488
www.jcb.org/cgi/doi/10.1083/jcb.201012088

Published August 1, 2011

their ability to interact with actin filaments in vitro (Altmann et al., 2008). Ypt11, a rab-like small GTPase, and Mmr1, an outer membrane protein of bud-localized mitochondria, were suggested to contribute to mitochondrial inheritance by interaction with Myo2 (Itoh et al., 2002, 2004; Frederick et al., 2008). These observations suggest that Myo2 drives anterograde mitochondrial movements in budding yeast and that this activity is supported by Ypt11 and Mmr1.

However, the role of Myo2 in mitochondrial transport and inheritance is controversial. It has been suggested that deletion of *YPT11* or mutations that compromise Myo2 have no significant effect on the velocity of mitochondrial movement. Instead, accumulation of mitochondria in the mother cells of *myo2*, *ypt11*, and *mmr1* mutants might be caused by defects in the retention of mitochondria at the bud tip (Boldogh et al., 2004; Boldogh and Pon, 2007; Pon, 2008; Peraza-Reyes et al., 2010). This scenario suggests an indirect role for Myo2 in mitochondrial transport, as the function of Myo2 would be limited to the transport of yet unknown retention factors to the bud tip, where they would prevent mitochondrial retrograde movement. An alternative Myo2-independent motility model suggests that mitochondria are moved by forces generated by Arp2/3-dependent actin polymerization and dynamics localized to the mitochondria via Jsn1 and Puf3, which are two members of the Puf family of RNA-binding proteins (Boldogh et al., 2001; Fehrenbacher et al., 2005; Boldogh and Pon, 2007; García-Rodríguez et al., 2007; Peraza-Reyes et al., 2010). A complex composed of three membrane proteins essential for mitochondrial distribution and morphology, Mdm10, Mdm12, and Mmm1, was proposed to link mitochondria to cytoskeletal tracks and provide directionality to Arp2/3-dependent movement (Boldogh et al., 2003; Boldogh and Pon, 2007; Peraza-Reyes et al., 2010). Thus, it is currently not clear whether bud-directed movement and inheritance of mitochondria are mediated by Myo2 or by motor-independent mechanisms or whether a contribution of both pathways is important (Valiathan and Weisman, 2008).

The analysis of the role of Myo2 in mitochondrial transport in vivo has been complicated by the fact that *MYO2* is an essential gene that is also required for numerous other cellular transport processes. Thus, *myo2* mutants always retain partial activity, and it may be difficult to discern direct from indirect effects. Here, we report on the construction of a mitochondria-specific Myo2 variant that contains a mitochondrial outer membrane anchor in place of the cargo binding domain. Functional analyses of this chimeric protein and detection of wild-type (WT) Myo2 on the mitochondrial surface by immuno-EM assign an essential role to Myo2 as a direct mediator of mitochondrial transport in budding yeast.

Results

Mutations in the Myo2 cargo binding domain affect mitochondrial distribution and morphology

The C-terminal globular cargo binding domain of Myo2 consists of two structurally and functionally discernible subdomains. The distal half contains binding sites for secretory vesicles and peroxisomes, whereas the proximal half interacts with vacuoles (Catlett et al., 2000; Pashkova et al., 2005b, 2006; Fagarasanu et al., 2009). We have previously shown that the vacuolar transport-defective alleles *myo2(Q1233R)* and *myo2(L1301P)* exhibit pronounced mitochondrial morphology and inheritance phenotypes (Altmann et al., 2008). To map the site on the Myo2 tail required for mitochondrial inheritance more precisely, we constructed a series of point mutants carrying amino acid exchanges in the vicinity of glutamine 1,233 and leucine 1,301: *myo2(L1229A)*, *myo2(T1230A)*, *myo2(K1234A)*, *myo2(V1235A)*, *myo2(V1236A)*, *myo2(T1237A)*, *myo2(E1293A)*, *myo2(Y1303A)*, *myo2(I1308A)*, and *myo2(P1529S)* (Fig. 1 A). Furthermore, we included the previously described alleles *myo2(G1248D)*,*myo2(D1297N)*,*myo2(D1297G)*,*myo2(N1304S)*, and *myo2(N1304D)* in our analysis (Catlett and Weisman, 1998; Catlett et al., 2000). As a control, we constructed two point mutants carrying amino acid substitutions on the backside of the subdomain, *myo2(K1538A)* and *myo2(F1542A)* (Fig. 1 A). Most mutant strains were observed to grow well on fermentable and nonfermentable carbon sources. However, *myo2(K1234A)* showed a pronounced growth defect, suggesting that the function of the cargo binding domain is more severely compromised (Fig. S1).

We analyzed mitochondrial distribution and morphology by fluorescence microscopy in *myo2* mutants expressing mitochondria-targeted (mt) GFP at 30 and 37°C. A significant number of cells contained abnormal mitochondria and/or buds devoid of mitochondria in all mutant strains (Fig. 1 B and Table S1). Similar, albeit not identical, effects were observed when the distribution of vacuoles was quantified after staining with CellTracker blue 7-amino-4-chloromethylcoumarin (CMAC; Table S1). Mitochondrial morphology and distribution defects were most severe when amino acid residues neighboring glutamine 1,233 and leucine 1,301 were mutated and were much less pronounced when amino acids on the backside of the subdomain were mutated (Fig. 1 A). We conclude that a region surrounding amino acid residues 1,233 and 1,301 on the proximal half of the Myo2 cargo binding domain is critical for anterograde mitochondrial transport. This region overlaps with the site critical for vacuolar transport.

Next, we combined the strong *myo2(Q1233R)* and *myo2(L1301P)* mutations in a single allele, *myo2(LQ)*. Western blotting of cell extracts confirmed that the steady-state protein levels of Myo2(Q1233R), Myo2(L1301P), and Myo2(LQ) were normal (Fig. S2 A). The *myo2(LQ)* mutant exhibited a more severe phenotype than either single mutant. It has a mild growth defect (Fig. S1), >90% of the cells have mitochondrial morphology defects, and ∼50% of the cells carry buds devoid of mitochondria (Fig. 1 B). To analyze the intracellular organization of mitochondria and the actin cytoskeleton, we stained mtGFP-expressing WT and *myo2(LQ)* mutant cells with rhodamine-phalloidin and analyzed them by confocal microscopy. Importantly, the actin cytoskeleton appeared normal in both WT and mutant cells (Fig. 1 C). In WT cells, tubular mitochondria are evenly distributed and often aligned along actin cables. In contrast, *myo2(LQ)* mutant mitochondria appear clumpy and aggregate in the mother cell opposite of the bud (Fig. 1 C). Thus, the *myo2(LQ)* mutant exhibits severe mitochondrial distribution and morphology defects.

Published August 1, 2011

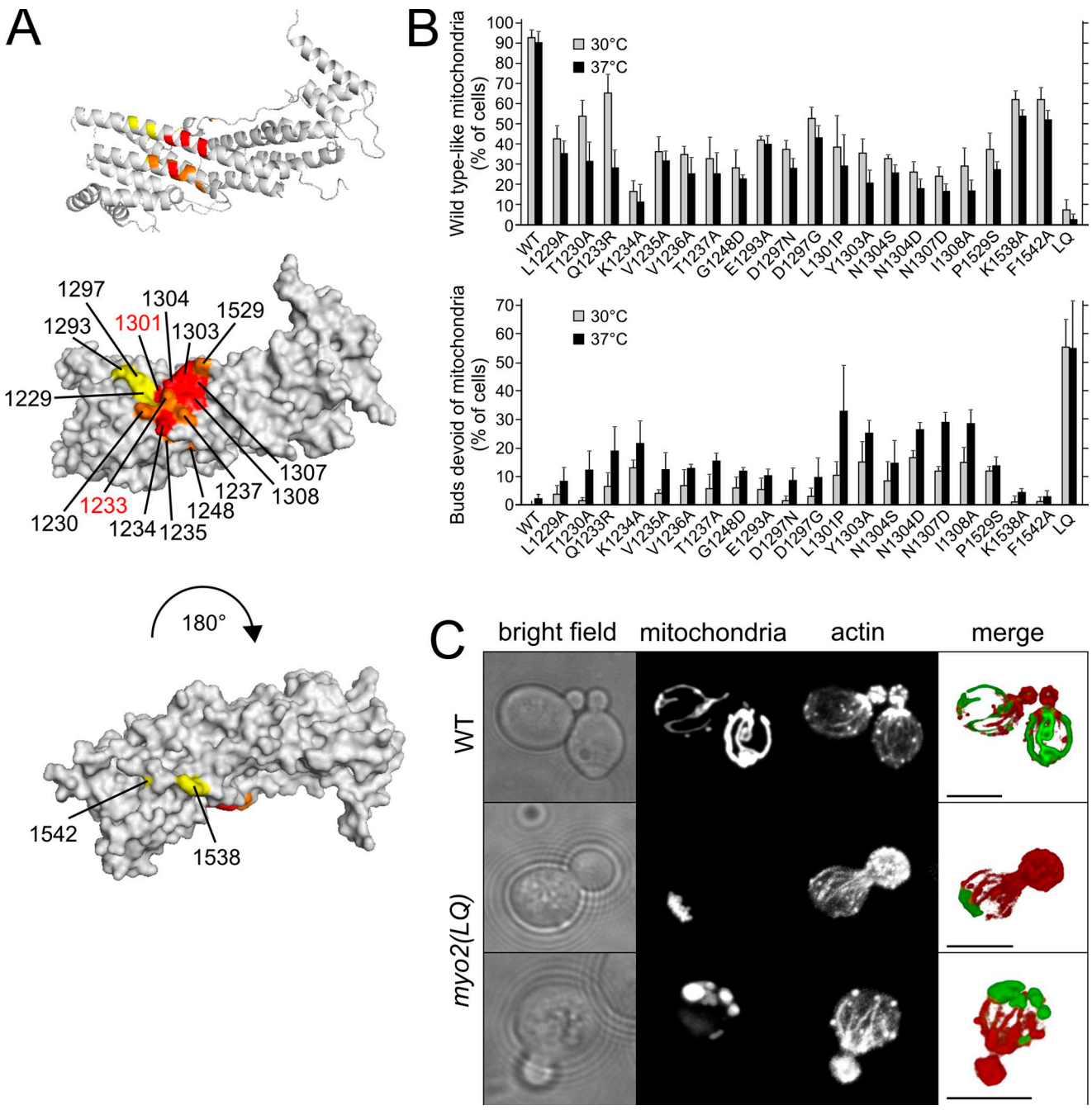

Figure 1. **Mutations in the proximal half of the Myo2 cargo binding domain produce mitochondrial distribution and morphology defects.** (A) Ribbon (top) and space-filling (middle and bottom) diagrams of the Myo2 tail structure were generated with PyMOL software (PyMOL Molecular Graphics System, version 1.3; Schrödinger). The locations of mutated amino acid residues are indicated. Residues L1301 and Q1233 mutated in the *myo2(LQ)* allele are highlighted in red. Residue V1236 is not indicated, as it is hidden in the interior of the domain. Red, >20% buds devoid of mitochondria; orange, 10–20% buds devoid of mitochondria; yellow, <10% buds devoid of mitochondria. (B) Cells were grown in yeast extract/peptone/dextrose (YPD) medium to the logarithmic growth phase and incubated for 3 h at the indicated temperature. Mitochondrial morphology (top) and buds devoid of mitochondria (bottom) were quantified at ambient temperature by fluorescence microscopy of mtGFP-expressing cells. Cells containing branched tubular mitochondria in the absence of any mitochondrial aggregation or fragmentation were classified as WT-like mitochondria. Quantifications are mean values from three independent experiments (n = 100), and error bars indicate standard deviations. (C) Cells expressing mtGFP were grown to the logarithmic growth phase in glucose-containing minimal medium, fixed, stained with rhodamine-phalloidin, and observed by confocal fluorescence microscopy. (left to right) Bright field image, maximum intensity projection of GFP fluorescence, maximum intensity projection of rhodamine fluorescence, and merged image generated with bioView3D software (The Center for Bio-Informatics, University of California, Santa Barbara, CA). Bars, 5 µm.

Published August 1, 2011

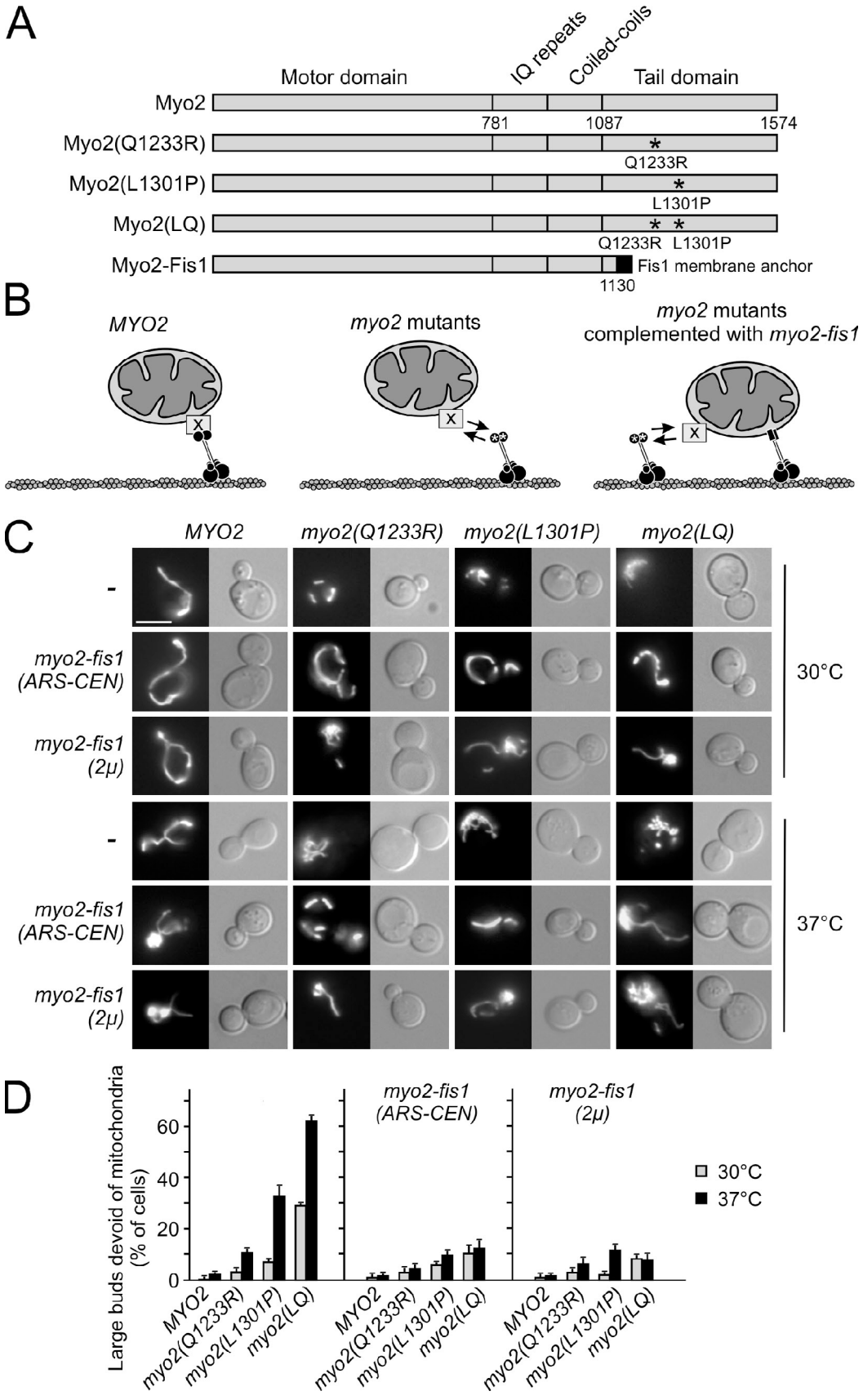

Figure 2. **Mitochondrial inheritance defects in *myo2* mutants are rescued by a mitochondria-specific Myo2 variant.** (A) Domain structure of WT and mutant Myo2 proteins. The numbers specify amino acid residues. Mutations are indicated by asterisks. (B) A schematic drawing of expected binding of Myo2 variants to mitochondria. (left) The WT Myo2 is thought to bind to a yet unidentified receptor (X) on the mitochondrial surface. (middle) Mutations

Published August 1, 2011

A mitochondrial membrane anchor replacing the Myo2 cargo binding domain restores mitochondrial distribution toward the bud in *myo2* mutants

The accumulation of mitochondria in the mother cell indicates that *myo2* mutations shift the balance of bidirectional anterograde and retrograde mitochondrial movements toward retrograde transport. This observation is compatible with both the mitochondrial motor model, which predicts that anterograde movements are impaired as a direct consequence of impaired Myo2 binding to mitochondria, and the retention factor model, which predicts that mutations of the Myo2 cargo binding domain impair transport of retention factors to the bud tip and increase the frequency of mitochondrial retrograde movement.

To discriminate between these models, we replaced the cargo binding domain of Myo2 (residues 1131–1574) with the C-terminal transmembrane segment of the tail-anchored mitochondrial outer membrane protein, Fis1 (residues 129–155; Fig. 2 A). This Fis1 segment is sufficient to anchor foreign proteins in the mitochondrial outer membrane (Kemper et al., 2008). It can be predicted that the chimeric protein Myo2-Fis1 is able to rescue *myo2* mutants that are directly impaired in binding of the motor to mitochondria but not the transport of retention factors to the bud (Fig. 2 B).

The *myo2-fis1* allele was placed under control of the *MYO2* promoter in low (*myo2-fis1(ARS-CEN)*) or multicopy (*myo2-fis1(2μ)*) plasmids. Intriguingly, the majority of *myo2(Q1233R)*, *myo2(L1301P)*, and *myo2(LQ)* mutant cells expressing Myo2-Fis1 from low copy plasmids contained WT-like mitochondria or exhibited only mild mitochondrial morphology defects (Fig. 2 C and Table S2), suggesting that the balance of anterograde and retrograde mitochondrial movements was restored. Expression of Myo2-Fis1 from a multicopy plasmid led to an accumulation of mitochondria in the bud (or at the bud neck in large-budded cells) and thus shifted the balance of bidirectional movements toward the anterograde direction (Fig. 2 C and Table S2). Whereas >95% of WT cells contained mitochondria in their buds under all conditions, up to 60% of large-budded *myo2* mutant cells (*myo2(LQ)* grown at 37°C) carried buds devoid of mitochondria. Partitioning of mitochondria to the bud was almost completely restored by expression of Myo2-Fis1 (Fig. 2 D). We conclude that mitochondrial distribution and morphology defects in *myo2(Q1233R)*, *myo2(L1301P)*, and *myo2(LQ)* mutants are not caused by the absence or mislocalization of retention factors but are a direct consequence of impaired binding of Myo2 to mitochondria.

Organelle specificity of *myo2(LQ)* and *myo2-fis1* alleles

To test whether the organellar distribution and morphology defects in the *myo2(LQ)* mutant are specific for mitochondria, we analyzed the distribution of other known Myo2 cargo organelles. Myo2-dependent polarized transport of secretory vesicles can be visualized by the accumulation of Sec4 at the tips of small buds (Schott et al., 1999), polarized distribution of Golgi cisternae in rapidly growing cells (Rossanese et al., 2001) can be examined with the late Golgi protein Sft2 (Conchon et al., 1999), and distribution of peroxisomes can be observed with fluorescent proteins carrying a PTS1 peroxisomal targeting signal (Smith et al., 2002; Fagarasanu et al., 2009). We found that the localization of secretory vesicles, Golgi, and peroxisomes to small buds was not altered in *myo2(LQ)* cells in comparison with the WT (Fig. 3 A). Thus, we conclude that the *myo2(LQ)* allele specifically affects the distribution of mitochondria and vacuoles. This is consistent with the fact that the region of Myo2 devoted to binding of secretory vesicles and peroxisomes is in the distal subdomain of the Myo2 tail (Pashkova et al., 2006; Fagarasanu et al., 2009). This region is distant from the proximal residues Q1233 and L1301, which appear to be critical for the transport of vacuoles and mitochondria (Pashkova et al., 2006; Altmann et al., 2008).

Mutations of amino acid residues to proline have the potential to perturb the structure of protein domains over long distances. However, the *myo2(L1301P)* mutation disrupts binding of Myo2 to its vacuolar receptor, Vac17, but not to Kar9 or Smy1, suggesting that *myo2(L1301P)* does not globally disrupt the Myo2 cargo binding domain (Pashkova et al., 2005a). As the intracellular distribution of secretory vesicles, Golgi, and peroxisomes is normal in *myo2(LQ)* cells, we conclude that the distal half of the Myo2 cargo binding domain is largely intact.

To date, there is no evidence for a role of Myo2 in ER inheritance. Accordingly, we found that the distribution of an ER marker carrying a signal sequence, a GFP moiety, and an ER retention signal (Prinz et al., 2000) was normal in *myo2(LQ)* cells (Fig. 3 B). As the ER and mitochondria are known to form relatively stable contacts (Kornmann et al., 2009), we asked whether inheritance of these organelles is coupled. It was already shown that *Δmyo4* mutant cells lacking cortical ER in the bud show normal inheritance of mitochondria (Estrada et al., 2003). Vice versa, we observed that *myo2(LQ)* mutant cells lacking mitochondria in the bud show normal inheritance of the ER (Fig. 3 C). As the *myo2(LQ)* allele affects the inheritance of both mitochondria and vacuoles (Table S1), we tested whether the inheritance of these organelles is coupled. We observed that the expression of Myo2-Fis1 in *myo2(LQ)* cells shifts the distribution of mitochondria toward the bud, whereas vacuoles remain in the mother cell (Fig. 3 D). These observations suggest that the inheritance of mitochondria is not coupled to the ER or vacuoles.

We also tested whether the activity of Myo2-Fis1 is specific for mitochondria. To confirm mitochondrial targeting,

in the Myo2 cargo binding domain (asterisks) are expected to weaken the interaction of Myo2 with mitochondria. (right) Myo2-Fis1 is directly inserted into the mitochondrial outer membrane through the Fis1 tail anchor and is expected to rescue cargo binding-defective *myo2* mutants. (C) Cells expressing mtGFP were grown in synthetic dextrose minimal medium to the logarithmic growth phase, incubated for 3 h at the indicated temperature, and analyzed by fluorescence microscopy at ambient temperature. (left) GFP fluorescence. (right) Differential interference contrast (DIC) image. Bar, 5 μm. (D) Cells were grown and analyzed as in C, and buds devoid of mitochondria were quantified in cells carrying large buds. Quantifications are mean values from three independent experiments (n = 100), and error bars indicate standard deviations.

Published August 1, 2011

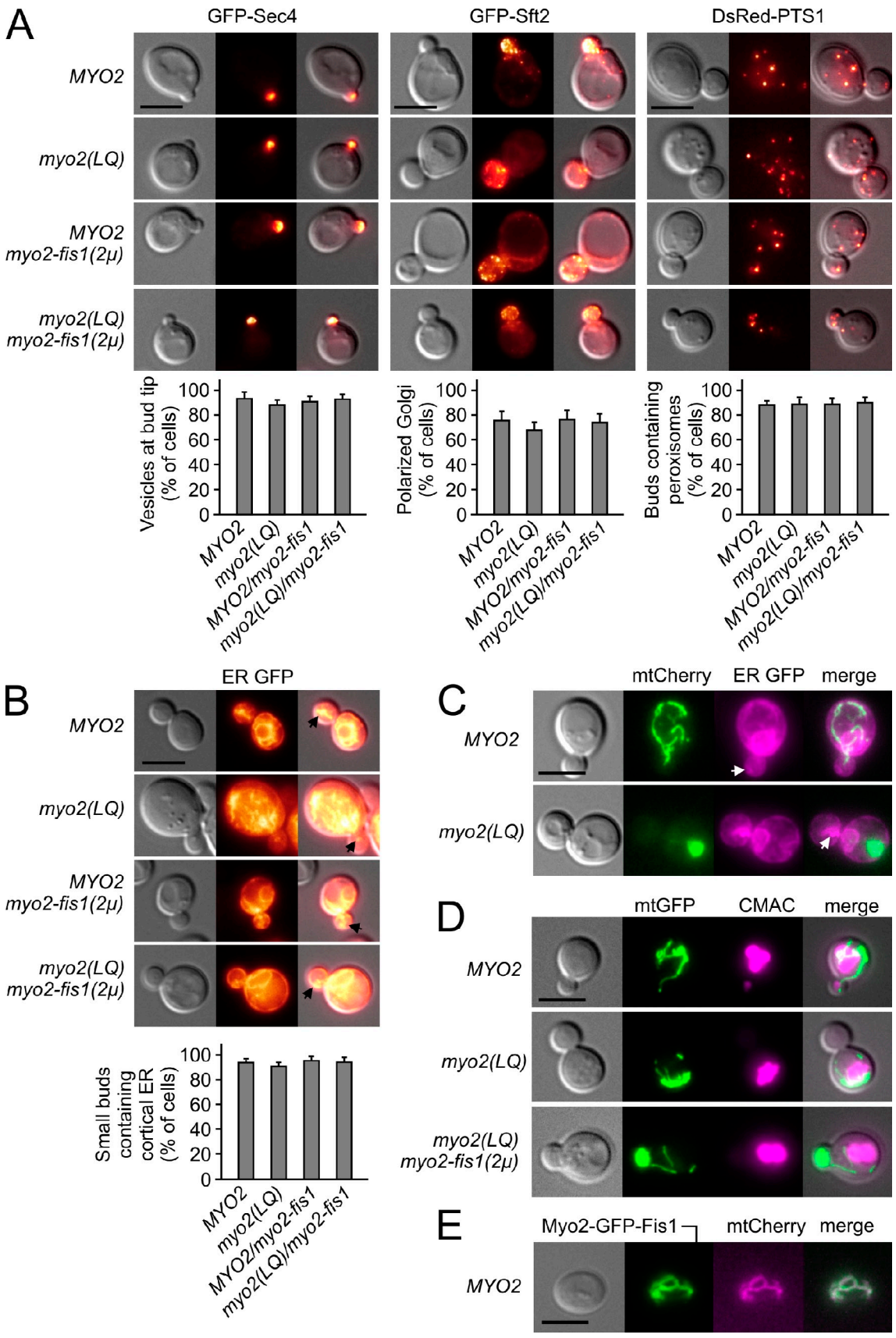

Figure 3. **Organelle specificity of *myo2* alleles.** (A) Cells were analyzed as in Fig. 2 C. (left) DIC of a representative cell. (middle) Maximum intensity projection of a z stack consisting of 10 focal planes. (right) Merge images. (B) Cells expressing a GFP marker for the ER were analyzed as in A with the exception that fluorescence images represent a single focal plane that is focused on the bud. Arrows indicate bud-localized ERs. (A and B) Quantifications are mean values from three independent experiments (n = 100), and error bars indicate standard deviations. (C) Cells coexpressing mtCherry and ER GFP

Published August 1, 2011

we constructed a Myo2-GFP-Fis1 variant that carries a GFP moiety inserted between the Myo2 and Fis1 segments. This construct was as efficient as the Myo2-Fis1 chimera in shifting mitochondrial distribution toward the bud (Fig. S2 B). Fluorescence microscopy of WT cells expressing Myo2-GFP-Fis1 revealed extensive colocalization of the GFP signal with mtCherry. Although most of the Myo2-GFP-Fis1 signal was concentrated in bud-localized mitochondria of polarized cells (Fig. S2 C), it was evenly distributed on the mitochondrial network in nonpolarized cells (Fig. 3 E), indicating correct insertion of the chimeric protein in the mitochondrial outer membrane. Expression of Myo2-Fis1 did not affect the intracellular distribution of secretory vesicles, Golgi, ER, and vacuoles (Fig. 3, A, B, and D). Also, in the case of peroxisomes, the percentage of organelle-containing buds was not changed by Myo2-Fis1 expression (Fig. 3 A). However, in some Myo2-Fis1–expressing cells, a shift of the intracellular distribution of peroxisomes from the mother cell toward the bud tip or the bud neck could be observed (~4% of the cells in a *MYO2* background and ~18% of the cells in a *myo2(LQ)* background). This can be explained by the fact that some Fis1 is targeted to peroxisomes (Motley et al., 2008). In summary, the expression of Myo2-Fis1 has a major effect on the intracellular distribution of mitochondria, a minor effect on peroxisomes, and no detectable effect on secretory vesicles, Golgi, ER, and vacuoles.

Entry of mitochondria into the bud is impaired in *myo2* mutants

We asked whether anterograde movement of mitochondria is directly compromised by mutation of the Myo2 cargo binding domain. To test this, we analyzed WT, *myo2(LQ)*, and *myo2-fis1(2µ)* cells by time-resolved 3D fluorescence microscopy in 16–27 cells per strain. We recorded z stacks of mtGFP-expressing cells by epifluorescence microscopy every 2 s and processed the images by deconvolution and maximum intensity projection. In WT cells, mitochondria were observed to undergo bidirectional movements both in the mother cell and the bud. *myo2(LQ)* mitochondria were motile, but their movements were restricted to the mother cell, and mitochondria rarely entered the bud. In contrast, *myo2-fis1(2µ)* mitochondria accumulated in the bud, and one or two long tubules were typically fixed at the opposite pole in the mother cell (Fig. S3 and Videos 1–3). These observations demonstrate that Myo2 is required for anterograde movement and entry of mitochondria into the bud.

It has been argued that Myo2 is not directly involved in anterograde mitochondrial movement because truncation of the Myo2 lever arm, predicted to attenuate transport velocity, was not found to have an effect on mitochondrial motility (Boldogh et al., 2004; Boldogh and Pon, 2007; Peraza-Reyes et al., 2010). We considered the possibility that factors other than motor-dependent velocity may also be important, such as cargo size,

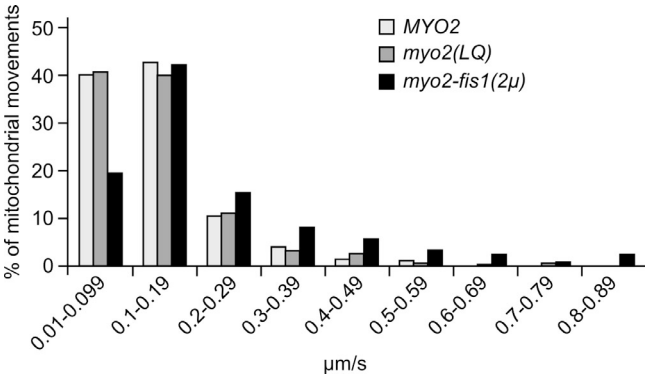

Figure 4. **Mitochondrial velocity is similar in WT, *myo2(LQ)*, and *myo2-fis1* strains.** *MYO2* WT, *myo2(LQ)* mutant, and *MYO2* cells expressing Myo2-Fis1 from a multicopy plasmid (*myo2-fis1(2µ)*) were grown to logarithmic growth phase in synthetic dextrose minimal medium and analyzed by time-resolved 3D fluorescence microscopy. Z stacks of mtGFP-expressing cells were recorded every 2 s and processed by deconvolution and maximum intensity projection. Representative cells are shown in Fig. S3 and Videos 1–3. A total number of 41 tracks of mitochondrial tips consisting of 276 time points were reconstructed in 27 WT cells, 50 tracks consisting of 341 time points in 25 *myo2(LQ)* mutant cells, and 28 tracks consisting of 123 time points in 16 *myo2-fis1(2µ)* mutant cells. For each time point, the 2D velocity was determined and expressed as a percentage of total mitochondrial movements for each strain.

number of motor molecules, ATP supply, etc. Based on our data, we reasoned that mitochondrial movements in the *myo2-fis1(2µ)* strain faithfully reflect Myo2-dependent mitochondrial velocity in vivo. If mitochondrial movements in WT and *myo2(LQ)* are similarly dependent on Myo2, they should occur with similar velocity. To test this, we used datasets obtained in the time-resolved 3D fluorescence microscopy experiment to determine mitochondrial velocities in WT, *myo2(LQ)*, and *myo2-fis1(2µ)* cells. We reconstructed tracks of mitochondrial tips and measured the velocity in 2D maximum intensity projections. The velocity of WT mitochondria was found to range from <0.1 to 0.9 µm/s with a strong bias toward slow motions (Fig. 4). These values are similar to previously reported observations (Fehrenbacher et al., 2004). Importantly, mitochondrial velocity was not significantly different in *myo2(LQ)* and *myo2-fis1(2µ)* cells (Fig. 4), suggesting that mitochondrial movements occur by the same mechanisms in all three strains.

Mitochondrial distribution and morphology defects in cells lacking Mmm1, Mdm10, Mdm12, or Mdm34 are not rescued by Myo2-Fis1

Mmm1, Mdm10, Mdm12, and Mdm34 are required for maintenance of normal mitochondrial distribution and morphology, cells lacking any one of these proteins contain spherical or clumped mitochondria that are immotile, buds are frequently devoid of mitochondria, and the mitochondrial genome is lost

were analyzed as in A. (right) Merged images of mCherry and GFP fluorescence. Arrows indicate bud-localized ERs. (D) Cells expressing mtGFP were stained with the vacuolar marker CMAC and analyzed as in A. (right) Merged images of GFP and CMAC fluorescence and DIC. (E) Cells coexpressing Myo2-GFP-Fis1 and mtCherry were grown to the late logarithmic growth phase and analyzed as in A. (right) A merged image of GFP and mCherry fluorescence. (C–E) Fluorescence images are maximum intensity projections of z stacks consisting of 10 focal planes. Bars, 5 µm.

Published August 1, 2011

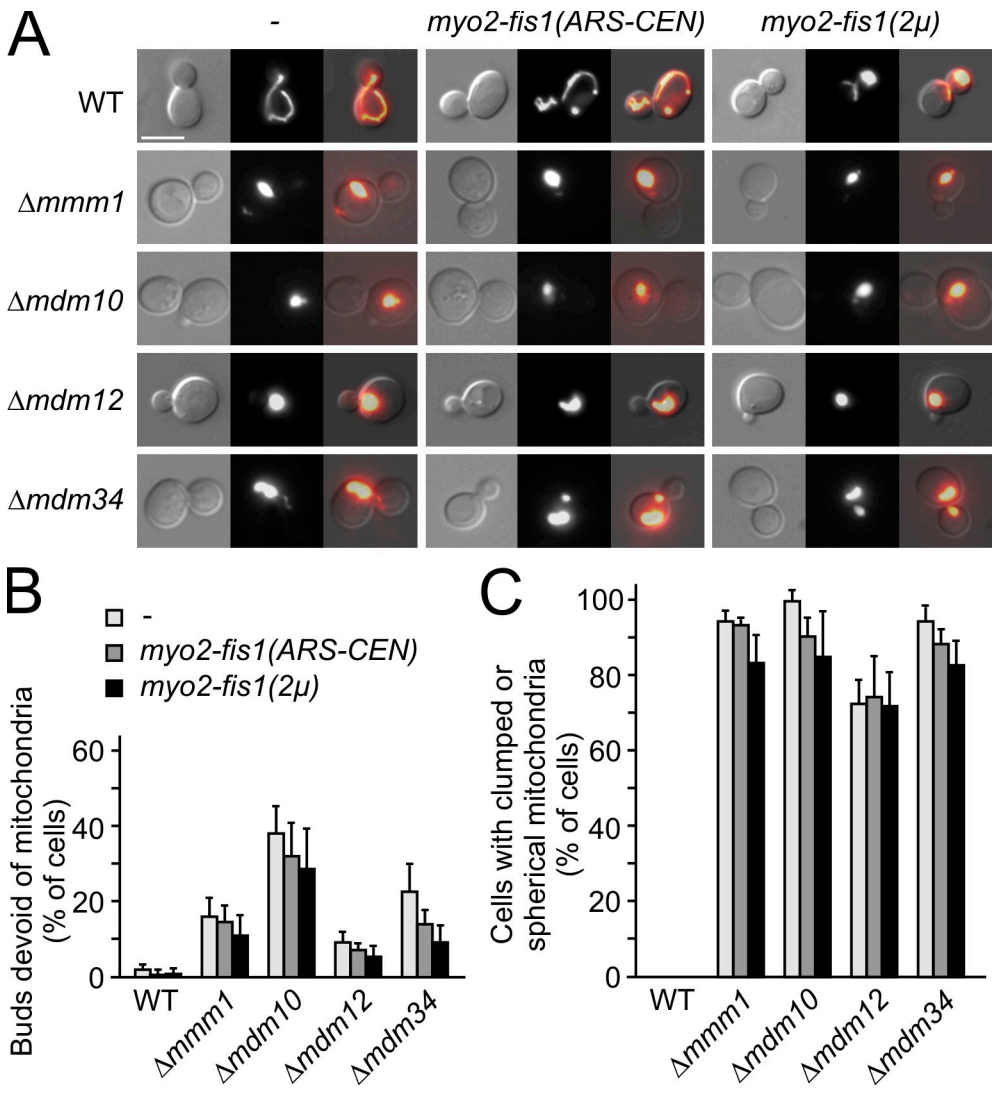

Figure 5. **Lack of Mmm1, Mdm10, Mdm12, or Mdm34 is not compensated by Myo2-Fis1.** (A) Cells expressing mtGFP were grown in synthetic dextrose minimal medium to the logarithmic growth phase and analyzed by fluorescence microscopy. (left) DIC image. (middle) GFP fluorescence. (right) Merged image. Bar, 5 µm. (B) Mitochondrial inheritance defects were quantified by counting buds devoid of mitochondria. (C) Mitochondrial morphology defects were quantified. (B and C) Quantifications are mean values from three independent experiments (n = 100), and error bars indicate standard deviations.

at high frequency (Burgess et al., 1994; Sogo and Yaffe, 1994; Berger et al., 1997; Boldogh et al., 1998, 2003; Dimmer et al., 2002; Youngman et al., 2004). It has been proposed that Mmm1, Mdm10, and Mdm12 link mitochondria to the cytoskeleton and contribute together with Myo2-independent forces to directed mitochondrial movements (Boldogh et al., 2003; Boldogh and Pon, 2007; Peraza-Reyes et al., 2010). We asked whether Myo2-Fis1 rescues mitochondrial distribution and morphology defects in *Δmmm1*, *Δmdm10*, *Δmdm12*, and *Δmdm34* mutants. Although WT cells transformed with the *myo2-fis1(2µ)* plasmid showed an accumulation of mitochondria in the bud, this could not be observed upon expression of Myo2-Fis1 in *Δmmm1*, *Δmdm10*, *Δmdm12*, and *Δmdm34* mutants. The majority of mutant cells contained abnormal mitochondria, and a significant number of cells carried buds devoid of mitochondria both in the presence and absence of the *myo2-fis1* plasmids (Fig. 5). Myo2-GFP-Fis1 colocalized with a mitochondrial matrix marker in *Δmmm1*, *Δmdm10*, *Δmdm12*, and *Δmdm34* cells (Fig. S2 D), suggesting that the failure of Myo2-Fis1 to rescue these mutants cannot be ascribed to a protein import defect. These observations suggest that defects in anterograde motility are not the primary cause for the mitochondrial distribution and morphology phenotypes in *Δmmm1*, *Δmdm10*, *Δmdm12*, and *Δmdm34* mutants.

myo2(Q1233R), *myo2(L1301P)*, and *myo2(LQ)* alleles interact genetically with *Δypt11*

Ypt11 is a small rab-type GTPase that has been suggested to cooperate with Myo2 in mitochondrial inheritance. It interacts with the tail domain of Myo2 in two-hybrid and coimmunoprecipitation experiments, and certain *myo2* mutant alleles genetically interact with the *Δypt11* deletion allele (Itoh et al., 2002). Overexpression of Ypt11 leads to the accumulation of mitochondria in the bud, suggesting that Ypt11 acts positively on anterograde mitochondrial movement (Itoh et al., 2002; Frederick et al., 2008).

Published August 1, 2011

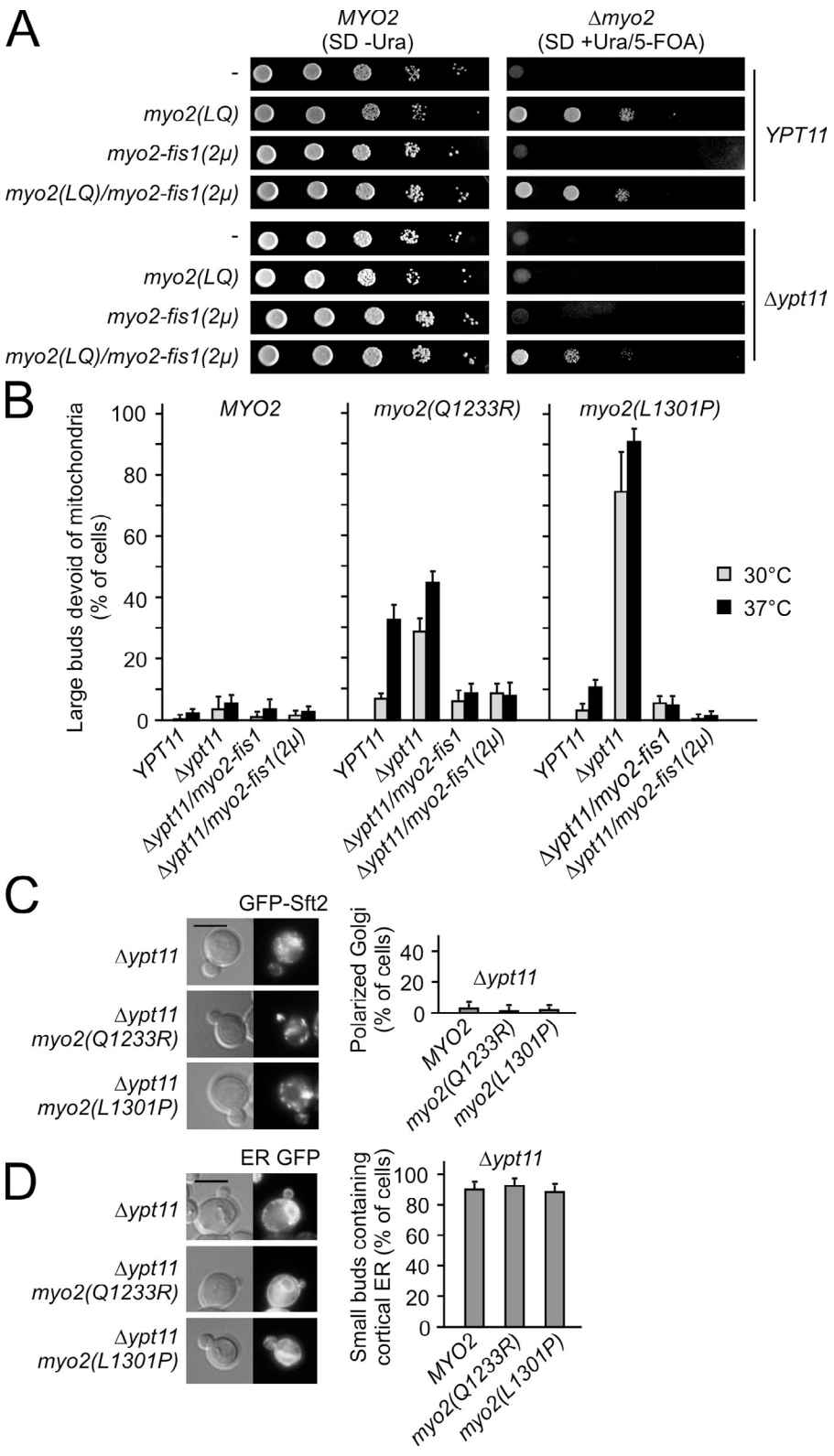

Figure 6. **Mutant alleles of the *MYO2* gene genetically interact with *Δypt11*.** (A) Growth was analyzed for strains carrying a chromosomal *myo2::kanMX4* deletion and the *MYO2* WT allele on a plasmid with a *URA3* marker together with empty vector (−), a *myo2(LQ)* plasmid, a *myo2-fis1(2μ)* plasmid, or both the *myo2(LQ)* plasmid and the *myo2-fis1(2μ)* plasmid either in a *YPT11* WT background (top) or a *Δypt11* deletion background (bottom). Cells were grown overnight in synthetic dextrose minimal medium containing uracil to allow for loss of the *URA3*-based *MYO2* plasmid. Then, 10-fold serial dilutions were spotted on synthetic dextrose plates lacking uracil (left) to allow growth of cells containing the *MYO2* WT plasmid or on synthetic dextrose plates containing uracil and 5-FOA (right) to select for cells that have lost the *MYO2* WT plasmid. SD − Ura plates were incubated for 3 d at 30°C, and SD + Ura/5-FOA plates were incubated for 5 d at 30°C. (B) Cells were grown and analyzed as in Fig. 2 D. Results are from the same series of experiments. (C) *Δypt11* cells carrying a chromosomal deletion of the *MYO2* gene contained plasmids expressing WT (*MYO2*), *myo2(Q1233R)*, or *myo2(L1301P)*. Cells expressing GFP-Sft2 were grown in synthetic dextrose minimal medium to the logarithmic growth phase and analyzed by fluorescence microscopy. (left) DIC image of a representative cell. (right) Maximum intensity projection of a z stack consisting of 10 focal planes. (D) Cells expressing ER GFP were analyzed as in C with the exception that fluorescence images represent a single focal plane that is focused on the bud. (B–D) Quantifications are mean values from three independent experiments (n = 100), and error bars indicate standard deviations. Bars, 5 μm.

We tested whether the *Δypt11* deletion genetically interacts with mitochondria-specific *myo2* mutant alleles. *YPT11* WT and *Δypt11* strains carrying chromosomal deletions of the *MYO2* gene and a WT copy on a plasmid with a *URA3* marker were transformed with plasmids expressing *myo2(LQ)* and/or *myo2-fis1(2μ)*. All strains were able to grow like WT as long as the *URA3* plasmid encoding WT *MYO2* was maintained (Fig. 6 A). Cells were cured from the *MYO2* plasmid by counterselection against the *URA3* marker on 5-fluoroorotic acid (5-FOA)–containing media. As expected, loss of this plasmid is lethal in control strains transformed with an empty vector and in strains transformed with *myo2-fis1(2μ)* plasmids (Fig. 6 A). The latter

Published August 1, 2011

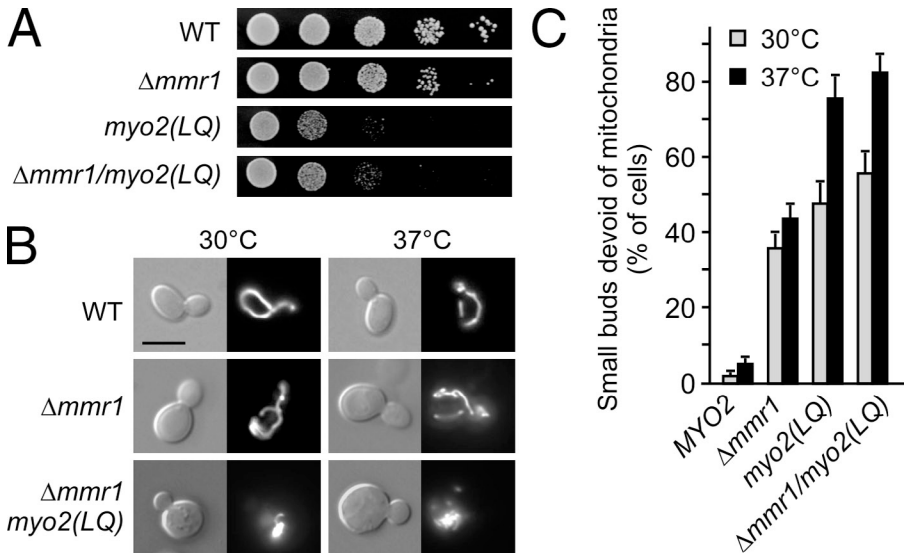

Figure 7. ***Δmmr1/myo2(LQ)* double mutant cells resemble *myo2(LQ)* single mutants.** (A) 10-fold serial dilutions of cell suspensions were spotted on yeast extract/peptone/dextrose plates and incubated at 30°C for 3 d. (B) Cells expressing mtGFP were grown at the indicated temperature in yeast extract/peptone/dextrose medium to the logarithmic growth phase and analyzed by fluorescence microscopy at ambient temperature. (left) DIC image. (right) GFP fluorescence. Bar, 5 µm. (C) Cells were grown as in B, and small buds devoid of mitochondria were quantified. Quantifications are mean values from three independent experiments (n = 100), and error bars indicate standard deviations.

result indicates that the mitochondria-specific Myo2-Fis1 chimera does not rescue essential functions of Myo2 in transport of other cell organelles and secretory vesicles. Cells containing the *myo2(LQ)* plasmid or the *myo2(LQ)* plasmid together with *myo2-fis1(2µ)* showed mild growth defects after loss of *MYO2* in the *YPT11* WT background (Fig. 6 A). However, the *myo2(LQ)* mutation is lethal in combination with the *Δypt11* allele (Fig. 6 A). This is consistent with the observations by Itoh et al. (2002), who reported synthetic lethality of *Δypt11* and the *myo2-573* allele, which has six mutations in the Myo2 tail. Synthetic lethality can occur by the combination of two nonessential mutations either in different pathways or in the same pathway (Boone et al., 2007). As Myo2 and Ypt11 physically interact with each other (Itoh et al., 2002), we consider it likely that they function in the same pathway. Intriguingly, viability of the *Δypt11/myo2(LQ)* double mutant was restored by expression of Myo2-Fis1 (Fig. 6 A). This suggests that lethality of *Δypt11/myo2(LQ)* can be ascribed to a lack of mitochondrial transport. We propose that Myo2-dependent mitochondrial transport is essential for viability in yeast.

Next, we tested whether the lack of Ypt11 produces synthetic mitochondrial phenotypes in the viable *Δypt11/myo2(Q1233R)* and *Δypt11/myo2(L1301P)* double mutants. We observed that defects of mitochondrial morphology and inheritance were exacerbated by deletion of the *YPT11* gene in *myo2(Q1233R)* and *myo2(L1301P)* mutants (Fig. 6 B and Table S2). Up to 90% of *Δypt11/myo2(L1301P)* cells carried buds devoid of mitochondria, compared with only 15% in *myo2(L1301P)* mutants in a *YPT11* WT background. Mitochondrial distribution and morphology defects could be efficiently rescued by the expression of Myo2-Fis1 (Fig. 6 B and Table S2). As *Δypt11* cells show a loss of polarized Golgi distribution (Arai et al., 2008) and a mild defect in the distribution of the ER (Buvelot Frei et al., 2006), we tested whether there are synthetic phenotypes for these organelles also. Consistent with the observations by Arai et al. (2008), we observed that late Golgi markers lost their polarized distribution in *Δypt11* cells; i.e., they were evenly distributed in mother and daughter cells. The distribution of late Golgi was very similar in *Δypt11/myo2(Q1233R)* and *Δypt11/myo2(L1301P)* cells compared with *Δypt11* single mutants (Fig. 6 C), suggesting that there are no synthetic defects in Golgi inheritance. Similarly, cortical ER was found in >90% of small buds of *myo2* mutant cells in the presence or absence of *YPT11* (Figs. 3 B and 6 D). These observations suggest that the *Δypt11* allele and the mutation *myo2(Q1233R)* or *myo2(L1301P)* produces synthetic mitochondrial phenotypes, whereas the inheritance of Golgi and ER is similar to that of *Δypt11* single mutants.

Deletion of the *MMR1* gene does not produce synthetic mitochondrial phenotypes in *myo2(LQ)*

Mmr1 is a protein of the mitochondrial outer membrane that was identified as a high copy suppressor of *myo2-573* (Itoh et al., 2004). Mmr1 is preferentially localized in mitochondria in the bud, forms a complex with Myo2, and promotes mitochondrial accumulation in the bud when overexpressed (Itoh et al., 2004; Frederick et al., 2008). It was proposed that Mmr1 and Ypt11 act independently of each other because the accumulation of mitochondria in buds upon Mmr1 overexpression does not require Ypt11 and vice versa (Itoh et al., 2004).

To test whether the *Δmmr1* deletion genetically interacts with *myo2(LQ)*, we constructed a double mutant and examined its phenotype. *Δmmr1/myo2(LQ)* cells are viable, and the growth defect of the *myo2(LQ)* single mutant is not enhanced by deletion of the *MMR1* gene (Fig. 7 A). Mitochondrial morphology in *Δmmr1* cells is almost like WT, whereas *Δmmr1/myo2(LQ)* mutant mitochondria are very similar to the *myo2(LQ)* single mutant (Fig. 7 B). We consider it unlikely that Mmr1 constitutes the mitochondrial receptor for Myo2 because *Δmmr1* cells exhibit only a mild mitochondrial inheritance phenotype. Consistent with the observations by Itoh et al. (2004), we found a significant mitochondrial inheritance defect in small buds of *Δmmr1* cells. This was more pronounced in *myo2(LQ)* mutants and not significantly further enhanced in *Δmmr1/myo2(LQ)*

Published August 1, 2011

double mutants (Fig. 7 C). Epistasis can be defined as a situation in which the activity of one gene masks effects at another locus, allowing inferences about the order of gene action (Boone et al., 2007). As the phenotype of the *Δmmr1/myo2(LQ)* double mutant is similar to that of the *myo2(LQ)* single mutant, we conclude that the *myo2(LQ)* allele is epistatic to *Δmmr1*. This suggests that Myo2 acts before Mmr1 in mitochondrial inheritance.

Myo2 is present on the mitochondrial surface

The evidence for a presence of Myo2 on mitochondria has been only indirect so far. For example, preincubation of purified mitochondria with antibodies against Myo2 abolishes binding of mitochondria to actin filaments in vitro, suggesting that the presence of Myo2 on mitochondria is important for this process (Altmann et al., 2008). However, immunofluorescence and GFP tagging studies have localized Myo2 mainly to cellular bud tips and bud necks (Lillie and Brown, 1994; Huh et al., 2003). Unfortunately, weak fluorescence signals and promiscuous binding of Myo2 to several cargoes do not allow a colocalization with mitochondria by fluorescence microscopy (unpublished data). Therefore, we tested a mitochondrial localization of Myo2 by immuno-EM. Mitochondria were isolated from WT cells by differential centrifugation and further purified by sucrose density gradient centrifugation. Purified mitochondria were fixed in glutaraldehyde and embedded in London Resin gold resin, and ultrathin sections were incubated with affinity-purified Myo2 antibodies and gold-coupled secondary antibodies and analyzed by transmission EM. Gold labeling was observed on the surface of organelles that could be clearly identified as mitochondria by their double membranes (Fig. 8 A). To test for the specificity of immunogold labeling, we extracted peripherally bound mitochondrial proteins with high salt or removed surface-exposed proteins by digestion with trypsin. These treatments are expected to reduce the number of Myo2 antigens per organelle. Finally, we isolated mitochondria from a *TetO$_7$-myo2* strain that carries the *MYO2* gene under control of a titratable promoter. Growth in the absence of doxycycline is expected to result in an overexpression of *MYO2*, whereas an addition of doxycycline to the medium represses the promoter and leads to depletion of Myo2 (Mnaimneh et al., 2004; Altmann et al., 2008). We observed that salt extraction, trypsin treatment, and repression of the *TetO$_7$-myo2* allele led to a reduction of labeling, whereas mitochondria isolated from Myo2-overexpressing cells showed excess labeling (Fig. 8 B and Table S3). We conclude that labeling is specific for Myo2 and that Myo2 is present on the surface of WT mitochondria.

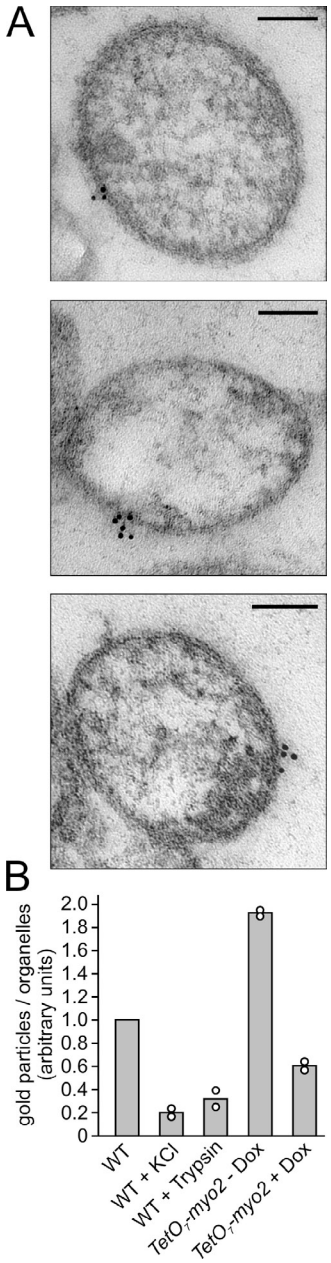

Figure 8. **Myo2 is present on mitochondria.** (A) Mitochondria were isolated from WT cells, purified by sucrose density centrifugation, and analyzed by postembedding immuno–EM using affinity-purified antibodies against Myo2. Bars, 100 nm. (B) WT mitochondria were either left untreated (WT), extracted with high salt (WT + KCl), or subjected to trypsin digestion (WT + trypsin). Mitochondria were purified from the *TetO$_7$-myo2* strain grown in the absence (*TetO$_7$-myo2* − Dox) or presence (*TetO$_7$-myo2* + Dox) of doxycycline. Mitochondria were analyzed by immuno–EM as in A. Between 106 and 341 mitochondria per sample were analyzed for the presence of gold particles. The number of gold particles per organelle was related to the untreated WT sample that was always analyzed in the same experiment. Results are mean values of two independent labeling experiments (Table S3). Individual data points are represented by circles.

Discussion

We constructed a novel *myo2* allele that has a selective and severe mitochondrial distribution phenotype, *myo2(LQ)*, and demonstrate that this can be rescued by the expression of a mitochondria-specific motor, Myo2-Fis1, pointing to a direct role of Myo2 in bud-directed mitochondrial transport. Furthermore, synthetic lethality of the *Δypt11/myo2(LQ)* double mutant is rescued by Myo2-Fis1. This suggests that mitochondrial inheritance cannot be maintained by Myo2-independent transport mechanisms. A direct role of Myo2 in mitochondrial transport is further supported by its detection on isolated WT mitochondria by immuno-EM. We propose that Myo2 mediates anterograde mitochondrial transport in yeast and that this activity is essential for viability.

Published August 1, 2011

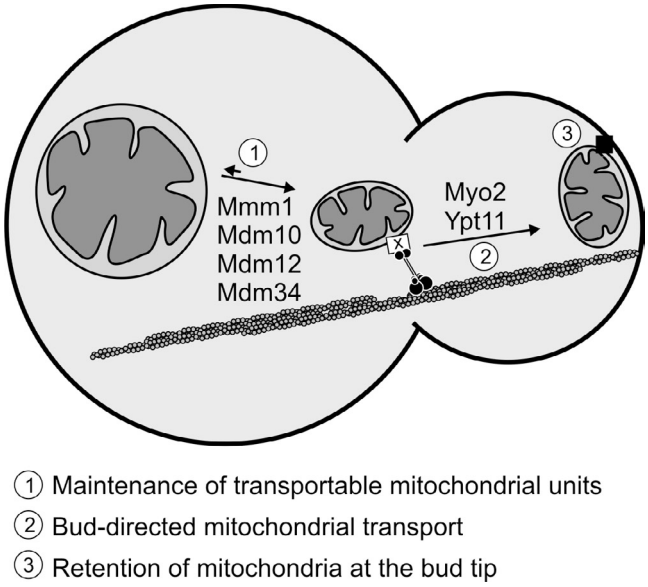

Figure 9. **Model of mitochondrial inheritance in yeast.** Anterograde movement is powered by Myo2 that is bound to mitochondria via a yet unknown receptor protein (X). The black square symbolizes hypothetical mitochondrial cortex anchors. See Discussion for details.

A function of Myo2 as a mitochondrial motor protein has repeatedly been questioned (Boldogh et al., 2004; Boldogh and Pon, 2007; Pon, 2008; Peraza-Reyes et al., 2010). It was argued that mutations of Myo2 have no effect on the velocity of mitochondrial movement. In particular, truncation of the Myo2 lever arm in the *myo2-Δ6IQ* mutant decreases the mean velocity of secretory vesicles from 3 to ∼0.3 µm/s (Schott et al., 2002), whereas mitochondria were observed to move at a speed of ∼0.18 µm/s both in WT and *myo2-Δ6IQ* cells (Boldogh et al., 2004). However, most mitochondrial movements that we observed were rather slow (<0.1 to 0.2 µm/s). As the speed of vesicles in *myo2-Δ6IQ* cells is still higher than that of mitochondria in WT cells, the velocity of mitochondria is apparently not solely determined by the speed of the motor. Thus, measurements of velocities in *myo2* mutants cannot be used to rule out Myo2 as a mitochondrial motor in yeast (Frederick and Shaw, 2007). Furthermore, it was suggested that the function of Myo2 is limited to the transport of mitochondrial retention factors to the bud (Boldogh et al., 2004; Boldogh and Pon, 2007; Pon, 2008; Peraza-Reyes et al., 2010). In this case, it would be expected that bud-directed Myo2-independent mitochondrial movements are not impaired in *myo2* mutants. We have previously examined mitochondrial motility in *myo2(L1301P)* cells over relatively long time periods at rather low temporal resolution (one z stack every 3 min over a total time of 30 min; Altmann et al., 2008). Here, we observed mitochondrial movements in *myo2(LQ)* cells with high temporal resolution (one z stack every 2 s over a total time of 1 min). In both cases, bidirectional mitochondrial movements could be observed in WT mother cells and buds. In contrast, mitochondria rarely passed the bud neck in *myo2* mutants. We conclude that mutations in the cargo binding domain of Myo2 directly impair bud-directed mitochondrial movement. It is expected that mutant Myo2 proteins retain some function in mitochondrial distribution, as a complete block of mitochondrial inheritance would be lethal. We propose that the frequency and/or distance of mitochondrial movements, but not their velocity, is compromised by mutations in the cargo binding domain in *myo2(L1301P)* and *myo2(LQ)* mutants.

Genetic evidence presented here and in other studies (Itoh et al., 2002, 2004; Boldogh et al., 2004; Frederick et al., 2008; Kornmann et al., 2009) allows us to propose a pathway of mitochondrial inheritance consisting of three sequential steps (Fig. 9). The first step of this pathway requires Mmm1, Mdm10, Mdm12, and Mdm34. Recently, these proteins were found to form a complex that tethers mitochondria with the ER and therefore was termed the ER-mitochondria encounter structure (ERMES; Kornmann et al., 2009). This complex is thought to facilitate interorganelle calcium and membrane lipid exchange (Kornmann et al., 2009; Wiedemann et al., 2009). These functions are expected to be independent of mitochondrial interactions with actin filaments. Here, we observed that mitochondrial distribution defects in ERMES complex mutants cannot be rescued by the expression of Myo2-Fis1. This suggests that Mmm1, Mdm10, Mdm12, and Mdm34 are required to maintain transportable mitochondrial units that are a prerequisite for directed transport along the cytoskeleton.

The second step of the mitochondrial inheritance pathway is bud-directed anterograde movement powered by Myo2. The complex formation of Ypt11 and Myo2 (Itoh et al., 2002) together with the synthetic mitochondrial phenotypes suggest that Ypt11 and Myo2 are required at the same step. Targeting of myosin V motors to their cargo organelles is often facilitated by rab-type GTPases (Hammer and Wu, 2002; Seabra and Coudrier, 2004; Akhmanova and Hammer, 2010). For example, Ypt11 supports binding of Myo2 to Ret2, a subunit of the COPI coatomer on Golgi compartments. Recruitment of Myo2 by this mechanism is important for bud-directed transport and inheritance of the Golgi (Arai et al., 2008). Our genetic observations support a model suggesting that Ypt11 cooperates with Myo2 in mitochondrial inheritance in a similar manner. In this scenario, Ypt11 might regulate binding of Myo2 to a yet unknown receptor on the mitochondrial surface. Binding of Myo2 to mitochondria may be impaired, albeit not blocked completely, by deletion of the *YPT11* gene or the mutation of the Myo2 cargo binding domain. A combination of both mutations is expected to weaken the interaction of the motor with the organelle even further. As a consequence, anterograde mitochondrial transport breaks down, resulting in a block of mitochondrial inheritance and a loss of viability. This lethal phenotype can be rescued by an expression of Myo2-Fis1 that bypasses the requirements of Ypt11 and an intact Myo2 cargo binding domain because it ensures mitochondrial targeting of Myo2 by the mitochondrial protein import machinery.

The third, and still rather hypothetical, step of the mitochondrial inheritance pathway is the retention of mitochondria in the bud. Mmr1 is an obvious candidate for this function, as its mRNA is localized to bud tips (Shepard et al., 2003), and the protein is highly enriched in bud-localized mitochondria (Itoh et al., 2004). Because most *Δmmr1* cells contain mitochondria

Published August 1, 2011

in their buds, it is conceivable that Mmr1 function may become important only after mitochondria have entered the bud. Possibly, Mmr1 of bud-localized mitochondria binds to bud tip–specific factors in the cell cortex and prevents backward movement of mitochondria to the mother cell. A function of Mmr1 downstream of Myo2 and Ypt11 is supported by our genetic data suggesting that the *myo2(LQ)* mutation is epistatic to *Δmmr1*. In other words, as long as mitochondria do not reach the bud tip, it is not important whether or not Mmr1 is present. However, a role of Mmr1 as a mitochondrial retention factor has not yet been demonstrated, and other proteins might play a role in immobilizing mitochondria in the bud. Although the available data clearly support a central role of Myo2 as a key component of mitochondrial inheritance, more work will be required to define the functions of ERMES complex components, Ypt11, and Mmr1 more precisely.

Myo2-powered transport of mitochondria in yeast may be taken as a paradigm for understanding myosin-mediated mitochondrial motility in higher organisms. Plant class XI myosins are closely related to fungal and metazoan class V myosins (Foth et al., 2006). Class XI myosins were found to colocalize with mitochondria in maize (Wang and Pesacreta, 2004) and are required for mitochondrial trafficking in leaf cells of tobacco (Avisar et al., 2008; Sparkes et al., 2008), and myosin inhibitors were shown to have an impact on mitochondrial movements in pollen tubes (Zheng et al., 2010). In metazoans, an unconventional myosin is associated with mitochondria in locust photoreceptor cells (Stürmer and Baumann, 1998), Myo19 is expressed in multiple tissues of vertebrates, localizes to mitochondria, and functions in actin-based mitochondrial motility (Quintero et al., 2009), and depletion of myosin V and VI in *Drosophila melanogaster* neurons augments microtubule-dependent mitochondrial motility, pointing to a role of myosins in organelle docking (Pathak et al., 2010). Collectively, these observations suggest that mitochondria-associated myosins are relatively common in higher organisms.

Materials and methods

Plasmids

Standard procedures were used for cloning and amplification of plasmids. Plasmid pVT100U-mtGFP, pYX142-mtGFP (Westermann and Neupert, 2000), or pYX142-mtCherry (provided by D. Scholz, Universität Bayreuth, Bayreuth, Germany) containing mCherry (Shaner et al., 2004) fused to the Su9 mitochondrial presequence was used to label mitochondria. Plasmid pDsRed-PTS1 (Smith et al., 2002) was used to label peroxisomes, and plasmid pWP1055 (Prinz et al., 2000) was used to label the ER. Plasmids pRS413-MYO2 (Catlett and Weisman, 1998) and pRS416-MYO2 (Catlett et al., 2000) were used to express the *MYO2* gene under control of its own regulatory elements. Novel mutant alleles containing single amino acid exchanges were constructed in pRS413-MYO2 using the QuikChange Site-Directed Mutagenesis kit (Agilent Technologies) according to the manufacturer's instructions and the primers listed in Table S4. The *myo2(LQ)* allele was constructed by mutagenesis of plasmid pRS413-myo2(L1301P) using primers Q1233Rfwd and Q1233Rrev. For construction of Myo2-Fis1 expression plasmids, an NheI site was removed in the vector backbone of pRS416-MYO2 using primers NheImutfwd and NheImutrev, and an NheI site was introduced in the *MYO2* coding region using primers NheIfwd and NheIrev. Then, the tail anchor coding region of the *FIS1* gene was amplified from genomic DNA by PCR using primers FIS1TMDfwd and FIS1TMDrev and cloned into the NheI and SacI sites of the modified plasmid, yielding pRS416-myo2-fis1. To obtain pRS413-myo2-fis1, pRS426-myo2-fis1, and pRS425-myo2-fis1, the *myo2-fis1* allele with its endogenous promoter was subcloned from pRS416-myo2-fis1 into the ClaI and SacI sites of pRS413 (Sikorski and Hieter, 1989) and pRS426 (Christianson et al., 1992) and the XhoI and SacI sites of pRS425 (Christianson et al., 1992). For construction of a Myo2-GFP-Fis1–expressing plasmid, pRS426-myo2-GFP-fis1, the GFP coding region was amplified from an mtGFP cassette using primers Myo2GFPfis1fwd and Myo2GFPfis1rev and cloned into the NheI site of pRS426-myo2-fis1. To obtain pYX142-GFP-Sft2 and pYX142-GFP-Sec4, the *SFT2* and *SEC4* coding sequences were amplified from genomic DNA using primers GFPSFT2fwd and GFPSFT2rev or GFPSEC4fwd and GFPSEC4rev, respectively, and cloned into the XhoI and BamHI sites of pYX142-GFPFIS1 (provided by D. Rapaport, University of Tübingen, Tübingen, Germany). Plasmid pGEX-4T-1 (Pashkova et al., 2006) was used for expression of the Myo2 tail domain in *Escherichia coli* for antibody production.

Yeast strains

Growth and manipulation of yeast strains were performed according to standard procedures (Sherman, 1991; Burke et al., 2000). The experiments shown in Figs. 1–7 and S1–3, Videos 1–3, and Tables S1 and S2 were performed with yeast strains isogenic to BY4741, BY4742, and BY4743 (Brachmann et al., 1998). To construct yeast strains expressing mutant *myo2* alleles, a haploid strain that contained a genomic *myo2::kanMX4* deletion allele and the *MYO2* WT allele on plasmid pRS416-MYO2 (Altmann et al., 2008) served as a recipient for pRS413-MYO2–derived plasmids containing *myo2* mutant alleles. After counterselection against pRS416-MYO2 by growth on 5-FOA–containing medium, strains were obtained that expressed *myo2* alleles from single-copy plasmids under control of the endogenous *MYO2* promoter. Double mutants were constructed by mating, sporulation, and tetrad dissection. For immuno-EM, mitochondria were isolated from the WT strain D273-10B (Sherman, 1964) and the *TetO$_7$-myo2* strain containing a titratable promoter allele (Mnaimneh et al., 2004).

Staining of cellular structures

Plasmids expressing mtGFP or mtCherry were used to visualize mitochondria, a plasmid expressing GFP-Sec4 was used to visualize secretory vesicles, a plasmid expressing GFP-Sft2 was used to label late Golgi cisternae, a plasmid expressing peroxisomal-targeted DsRed was used to label peroxisomes, and a plasmid expressing ER-targeted GFP was used to label the ER. The actin cytoskeleton was stained with rhodamine-phalloidin (Invitrogen) as previously described (Amberg, 1998). In brief, cells were grown to the logarithmic growth phase in synthetic dextrose medium, fixed with 4% formaldehyde for 10 min at room temperature, washed with PBS, stained for 1 h under agitation with rhodamine-phalloidin according to the manufacturer's instructions, washed with PBS, and subjected to fluorescence microscopy. Vacuoles were stained with CellTracker blue CMAC (Invitrogen) according to the manufacturer's instructions. In brief, cells were grown to the logarithmic growth phase in synthetic dextrose medium, incubated with 100 µM CMAC for 20 min under agitation at 30°C, washed with synthetic dextrose medium, and subjected to fluorescence microscopy.

Light microscopy

Cells were immobilized in 0.5% low melting point agarose in growth medium. Confocal fluorescence microscopy images in Fig. 1 C were obtained using a true confocal scanner spectrophotometer system (Leica) in combination with a DM IRBE inverted microscope equipped with a 100×/1.40 HCX PL APO oil objective (Leica). Epifluorescence images in Figs. 2 C, 5 A, and 7 B and data in Figs. 1 B, 2 D, 3 (A and B), 5 (B and C), 6 (B–D), and 7 C and Tables S1 and S2 were obtained at ambient temperature with a microscope (Axioplan 2; Carl Zeiss) equipped with a Plan Neofluar 100×/1.30 Ph3 oil objective (Carl Zeiss). Images were recorded with a monochrome camera (Evolution VF Mono Cooled; Intas) and processed with Image-Pro Plus 5.0 and Scope-Pro 4.5 software (Media Cybernetics). Time-resolved epifluorescence images and data in Figs. 4 and S3 and Videos 1–3 were obtained with an inverted microscope (DMI6000 B; Leica) equipped with a 100×/1.40 HCX PL APO oil objective and a monochrome camera (DFC360 FX; Leica). The temperature was 30°C and was controlled with Inkubator BL (PeCon GmbH). Images were obtained with AF 6000 Core software (Leica) and subjected to deconvolution with 3D deconvolution LAS AF software (AF6000; Leica). Merged images and mitochondrial tracks were generated with ImageJ software (version 1.43; National Institutes of Health; Abramoff et al., 2004). Epifluorescence images in Figs. 3, 6 (C and D), and S2 B were obtained at ambient temperature with the same microscope and AF6000 Core software. Fluorescence is shown in false color. CorelDRAW Graphics Suite software (version 12.0; Corel Corporation) was used for mounting of the figures; image manipulations other than minor adjustments of brightness and contrast were

not performed. If not indicated otherwise, quantifications are mean values from three independent experiments (n = 100), and error bars indicate standard deviations.

All datasets within a given figure were obtained in the same series of experiments performed under identical experimental conditions and can be directly compared. However, it should be noted that quantifications obtained in different series of experiments or by different researchers in different studies should be compared with caution. In some experiments, different growth media and/or genetic strain backgrounds were used, there might have been variations in the temperature during microscopy, and different morphological classes may have been used to quantify subtle phenotypes. In some experiments, mitochondrial phenotypes were specifically quantified in large and/or small buds (as indicated in the figure legends).

Antibodies

The Myo2 tail domain (amino acids 1131–1575) was expressed as a GST fusion protein in *E. coli* and purified as previously described (Pashkova et al., 2006). In brief, bacterial cells were lysed in the presence of protease inhibitors by repeated freeze-thaw cycles and sonication, and soluble protein was bound to glutathione–Sepharose 4B (GE Healthcare) and eluted by thrombin cleavage (Thrombin Cleavage Capture kit; EMD). Thrombin was removed by addition of streptavidin agarose beads, and the purified protein was injected into rabbits (BioGenes). Affinity purification of the serum was performed with antigen coupled to cyanogen bromide–activated Sepharose as previously described (Harlow and Lane, 1999). Western blotting was performed according to standard procedures.

Preparation of cell extracts, isolation, and manipulation of mitochondria

Spheroplasts were prepared according to Altmann et al. (2007) and dissolved in SDS sample buffer to generate cell extracts. Induction and repression of the *TetO$_7$-myo2* promoter allele before isolation of mitochondria were performed as previously described (Altmann et al., 2008). Mitochondria were isolated by differential centrifugation and sucrose gradient purification according to published procedures (Altmann et al., 2007). For high salt extraction, mitochondria were resuspended in SEM buffer (250 mM sucrose, 1 mM EDTA, and 10 mM MOPS/KOH, pH 7.4) supplemented with 1 M KCl, incubated for 30 min on ice, pelleted by centrifugation for 3 min at 18,000 *g* at 4°C, washed with SEM, and centrifuged again. Protease treatment was performed by an addition of 50 µg/ml trypsin to mitochondria suspended in SEM and by incubation for 15 min on ice. Protease treatment was stopped by an addition of 200 µg/ml soybean trypsin inhibitor and by incubation for 5 min on ice. Mitochondria were pelleted by centrifugation for 3 min at 18,000 *g* at 4°C, washed with SEM, and centrifuged again. Mitochondrial pellets were used for preparation for immuno-EM.

Postembedding immuno-EM

Pellets of isolated mitochondria were fixed for 30 min at room temperature in 1% glutaraldehyde in 100 mM cacodylate buffer, pH 7.2. Samples were dehydrated on ice in ethanol using 10% increments up to 70% ethanol for 20 min each followed by 10% increments at −20°C up to 100% ethanol. Mitochondria were infiltrated, embedded in gold resin (London Resin Co. Ltd.) in 10% increments for 20 min each at −20°C, and polymerized for 3 d with UV light at −20°C. Blocks were then hardened with daylight for another 24 h at room temperature. Ultrathin 60-nm sections were cut with a diamond knife (type ultra 35°; Diatome) on an ultramicrotome (Ultracut UCT; Leica) and prepared for immunolabeling immediately afterward. Grids were incubated at room temperature on 1% acetylated BSA (Aurion) for 30 min, placed on 0.1% acetylated BSA in PBS containing 0.1% glycine for 15 min, and washed three times on 0.1% acetylated BSA in PBS. Grids were placed on droplets containing affinity-purified antibodies against Myo2 at a dilution of 1:100 in PBS buffer containing 0.1% acetylated BSA and incubated overnight at 4°C. After two washes in PBS/0.1% acetylated BSA, samples were transferred to 10-nm gold-coupled secondary antibodies (BBInternational) at a dilution of 1:50 in PBS supplemented with 0.1% acetylated BSA and incubated for 90 min at room temperature. After three washes on 0.1% acetylated BSA in PBS and three washes on H_2O (15 min each), sections were poststained at room temperature with 2% uranyl acetate in H_2O (10–15 min) and lead citrate (3–5 min; Reynolds, 1963). Samples were examined in a transmission electron microscope (JEM-2100; JEOL Ltd.) operated at 80 kV. Micrographs were taken using a 4,080 × 4,080–pixel charge-coupled device camera (UltraScan 4000; Gatan, Inc) and digital micrograph software (version 1.70.16; Gatan, Inc).

Online supplemental material

Fig. S1 shows growth behavior of *myo2* mutants. Fig. S2 shows steady-state levels of mutant Myo2 proteins and mitochondrial targeting of Myo2-GFP-Fis1. Fig. S3 shows mitochondrial movements in WT, *myo2(LQ)*, and *myo2-fis1* strains. Videos 1–3 show mitochondrial movements in a WT cell (Video 1), a *myo2(LQ)* cell (Video 2), and a *myo2-fis1(2µ)* cell (Video 3). Table S1 shows mitochondrial and vacuolar inheritance defects in *myo2* mutants. Table S2 shows mitochondrial morphology defects in *myo2* mutants. Table S3 shows quantification of Myo2 immunolabeling on isolated mitochondria. Table S4 lists the primers used in this study. Online supplemental material is available at http://www.jcb.org/cgi/content/full/jcb.201012088/DC1.

We thank Annette Suske and Rita Grotjahn for technical assistance, Markus Hermann for help with antibody purification, Stefan Geimer for advice with EM, Till Klecker for helpful discussions, and students Philipp Schmid and Evelin Urban for their contributions to some experiments. We are grateful to William A. Prinz, Richard A. Rachubinski, Doron Rapaport, Dirk Scholz, and Lois S. Weisman for making plasmids available to us.

This work was supported by Deutsche Forschungsgemeinschaft through grant DFG We 2174/3-3.

Submitted: 14 December 2010
Accepted: 6 July 2011

References

Abramoff, M.D., P.J. Magelhaes, and S.J. Ram. 2004. Image processing with ImageJ. *Biophot. Int.* 11:36–42.

Akhmanova, A., and J.A. Hammer III. 2010. Linking molecular motors to membrane cargo. *Curr. Opin. Cell Biol.* 22:479–487. doi:10.1016/j.ceb.2010.04.008

Altmann, K., and B. Westermann. 2005. Role of essential genes in mitochondrial morphogenesis in *Saccharomyces cerevisiae*. *Mol. Biol. Cell*. 16:5410–5417. doi:10.1091/mbc.E05-07-0678

Altmann, K., M. Dürr, and B. Westermann. 2007. *Saccharomyces cerevisiae* as a model organism to study mitochondrial biology: general considerations and basic procedures. *Methods Mol. Biol.* 372:81–90. doi:10.1007/978-1-59745-365-3_6

Altmann, K., M. Frank, D. Neumann, S. Jakobs, and B. Westermann. 2008. The class V myosin motor protein, Myo2, plays a major role in mitochondrial motility in *Saccharomyces cerevisiae*. *J. Cell Biol.* 181:119–130. doi:10.1083/jcb.200709099

Amberg, D.C. 1998. Three-dimensional imaging of the yeast actin cytoskeleton through the budding cell cycle. *Mol. Biol. Cell*. 9:3259–3262.

Arai, S., Y. Noda, S. Kainuma, I. Wada, and K. Yoda. 2008. Ypt11 functions in bud-directed transport of the Golgi by linking Myo2 to the coatomer subunit Ret2. *Curr. Biol.* 18:987–991. doi:10.1016/j.cub.2008.06.028

Avisar, D., A.I. Prokhnevsky, K.S. Makarova, E.V. Koonin, and V.V. Dolja. 2008. Myosin XI-K Is required for rapid trafficking of Golgi stacks, peroxisomes, and mitochondria in leaf cells of *Nicotiana benthamiana*. *Plant Physiol.* 146:1098–1108. doi:10.1104/pp.107.113647

Berger, K.H., L.F. Sogo, and M.P. Yaffe. 1997. Mdm12p, a component required for mitochondrial inheritance that is conserved between budding and fission yeast. *J. Cell Biol.* 136:545–553. doi:10.1083/jcb.136.3.545

Boldogh, I.R., and L.A. Pon. 2007. Mitochondria on the move. *Trends Cell Biol.* 17:502–510. doi:10.1016/j.tcb.2007.07.008

Boldogh, I., N. Vojtov, S. Karmon, and L.A. Pon. 1998. Interaction between mitochondria and the actin cytoskeleton in budding yeast requires two integral mitochondrial outer membrane proteins, Mmm1p and Mdm10p. *J. Cell Biol.* 141:1371–1381. doi:10.1083/jcb.141.6.1371

Boldogh, I.R., H.-C. Yang, W.D. Nowakowski, S.L. Karmon, L.G. Hays, J.R. Yates III, and L.A. Pon. 2001. Arp2/3 complex and actin dynamics are required for actin-based mitochondrial motility in yeast. *Proc. Natl. Acad. Sci. USA*. 98:3162–3167. doi:10.1073/pnas.051494698

Boldogh, I.R., D.W. Nowakowski, H.C. Yang, H. Chung, S. Karmon, P. Royes, and L.A. Pon. 2003. A protein complex containing Mdm10p, Mdm12p, and Mmm1p links mitochondrial membranes and DNA to the cytoskeleton-based segregation machinery. *Mol. Biol. Cell*. 14:4618–4627. doi:10.1091/mbc.E03-04-0225

Boldogh, I.R., S.L. Ramcharan, H.C. Yang, and L.A. Pon. 2004. A type V myosin (Myo2p) and a Rab-like G-protein (Ypt11p) are required for retention of newly inherited mitochondria in yeast cells during cell division. *Mol. Biol. Cell*. 15:3994–4002. doi:10.1091/mbc.E04-01-0053

Boone, C., H. Bussey, and B.J. Andrews. 2007. Exploring genetic interactions and networks with yeast. *Nat. Rev. Genet.* 8:437–449. doi:10.1038/nrg2085

Brachmann, C.B., A. Davies, G.J. Cost, E. Caputo, J. Li, P. Hieter, and J.D. Boeke. 1998. Designer deletion strains derived from *Saccharomyces*

cerevisiae S288C: a useful set of strains and plasmids for PCR-mediated gene disruption and other applications. *Yeast*. 14:115–132. doi:10.1002/(SICI)1097-0061(19980130)14:2<115::AID-YEA204>3.0.CO;2-2

Bretscher, A. 2003. Polarized growth and organelle segregation in yeast: the tracks, motors, and receptors. *J. Cell Biol.* 160:811–816. doi:10.1083/jcb.200301035

Burgess, S.M., M. Delannoy, and R.E. Jensen. 1994. *MMM1* encodes a mitochondrial outer membrane protein essential for establishing and maintaining the structure of yeast mitochondria. *J. Cell Biol.* 126:1375–1391. doi:10.1083/jcb.126.6.1375

Burke, D., D. Dawson, and T. Stearns. 2000. Methods in Yeast Genetics: a Cold Spring Harbor Laboratory Course Manual. Cold Spring Harbor Laboratory Press, Plainview, NY. 205 pp.

Buvelot Frei, S., P.B. Rahl, M. Nussbaum, B.J. Briggs, M. Calero, S. Janeczko, A.D. Regan, C.Z. Chen, Y. Barral, G.R. Whittaker, and R.N. Collins. 2006. Bioinformatic and comparative localization of Rab proteins reveals functional insights into the uncharacterized GTPases Ypt10p and Ypt11p. *Mol. Cell. Biol.* 26:7299–7317. doi:10.1128/MCB.02405-05

Catlett, N.L., and L.S. Weisman. 1998. The terminal tail region of a yeast myosin-V mediates its attachment to vacuole membranes and sites of polarized growth. *Proc. Natl. Acad. Sci. USA*. 95:14799–14804. doi:10.1073/pnas.95.25.14799

Catlett, N.L., and L.S. Weisman. 2000. Divide and multiply: organelle partitioning in yeast. *Curr. Opin. Cell Biol.* 12:509–516. doi:10.1016/S0955-0674(00)00124-1

Catlett, N.L., J.E. Duex, F. Tang, and L.S. Weisman. 2000. Two distinct regions in a yeast myosin-V tail domain are required for the movement of different cargoes. *J. Cell Biol.* 150:513–526. doi:10.1083/jcb.150.3.513

Christianson, T.W., R.S. Sikorski, M. Dante, J.H. Shero, and P. Hieter. 1992. Multifunctional yeast high-copy-number shuttle vectors. *Gene*. 110:119–122. doi:10.1016/0378-1119(92)90454-W

Conchon, S., X. Cao, C. Barlowe, and H.R. Pelham. 1999. Got1p and Sft2p: membrane proteins involved in traffic to the Golgi complex. *EMBO J.* 18:3934–3946. doi:10.1093/emboj/18.14.3934

Dimmer, K.S., S. Fritz, F. Fuchs, M. Messerschmitt, N. Weinbach, W. Neupert, and B. Westermann. 2002. Genetic basis of mitochondrial function and morphology in *Saccharomyces cerevisiae*. *Mol. Biol. Cell*. 13:847–853. doi:10.1091/mbc.01-12-0588

Estrada, P., J. Kim, J. Coleman, L. Walker, B. Dunn, P. Takizawa, P. Novick, and S. Ferro-Novick. 2003. Myo4p and She3p are required for cortical ER inheritance in *Saccharomyces cerevisiae*. *J. Cell Biol.* 163:1255–1266. doi:10.1083/jcb.200304030

Fagarasanu, A., and R.A. Rachubinski. 2007. Orchestrating organelle inheritance in *Saccharomyces cerevisiae*. *Curr. Opin. Microbiol.* 10:528–538. doi:10.1016/j.mib.2007.10.002

Fagarasanu, A., F.D. Mast, B. Knoblach, Y. Jin, M.J. Brunner, M.R. Logan, J.N. Glover, G.A. Eitzen, J.D. Aitchison, L.S. Weisman, and R.A. Rachubinski. 2009. Myosin-driven peroxisome partitioning in *S. cerevisiae*. *J. Cell Biol.* 186:541–554. doi:10.1083/jcb.200904050

Fagarasanu, A., F.D. Mast, B. Knoblach, and R.A. Rachubinski. 2010. Molecular mechanisms of organelle inheritance: lessons from peroxisomes in yeast. *Nat. Rev. Mol. Cell Biol.* 11:644–654. doi:10.1038/nrm2960

Fehrenbacher, K.L., H.C. Yang, A.C. Gay, T.M. Huckaba, and L.A. Pon. 2004. Live cell imaging of mitochondrial movement along actin cables in budding yeast. *Curr. Biol.* 14:1996–2004. doi:10.1016/j.cub.2004.11.004

Fehrenbacher, K.L., I.R. Boldogh, and L.A. Pon. 2005. A role for Jsn1p in recruiting the Arp2/3 complex to mitochondria in budding yeast. *Mol. Biol. Cell*. 16:5094–5102. doi:10.1091/mbc.E05-06-0590

Foth, B.J., M.C. Goedecke, and D. Soldati. 2006. New insights into myosin evolution and classification. *Proc. Natl. Acad. Sci. USA*. 103:3681–3686. doi:10.1073/pnas.0506307103

Frederick, R.L., and J.M. Shaw. 2007. Moving mitochondria: establishing distribution of an essential organelle. *Traffic*. 8:1668–1675. doi:10.1111/j.1600-0854.2007.00644.x

Frederick, R.L., K. Okamoto, and J.M. Shaw. 2008. Multiple pathways influence mitochondrial inheritance in budding yeast. *Genetics*. 178:825–837. doi:10.1534/genetics.107.083055

García-Rodríguez, L.J., A.C. Gay, and L.A. Pon. 2007. Puf3p, a Pumilio family RNA binding protein, localizes to mitochondria and regulates mitochondrial biogenesis and motility in budding yeast. *J. Cell Biol.* 176:197–207. doi:10.1083/jcb.200606054

Hammer, J.A. III, and X.S. Wu. 2002. Rabs grab motors: defining the connections between Rab GTPases and motor proteins. *Curr. Opin. Cell Biol.* 14:69–75. doi:10.1016/S0955-0674(01)00296-4

Harlow, E., and D. Lane. 1999. Using Antibodies: A Laboratory Manual. Cold Spring Harbor Laboratory Press, Cold Spring Harbor, NY. 495 pp.

Huh, W.K., J.V. Falvo, L.C. Gerke, A.S. Carroll, R.W. Howson, J.S. Weissman, and E.K. O'Shea. 2003. Global analysis of protein localization in budding yeast. *Nature*. 425:686–691. doi:10.1038/nature02026

Itoh, T., A. Watabe, A. Toh-E, and Y. Matsui. 2002. Complex formation with Ypt11p, a rab-type small GTPase, is essential to facilitate the function of Myo2p, a class V myosin, in mitochondrial distribution in *Saccharomyces cerevisiae*. *Mol. Cell. Biol.* 22:7744–7757. doi:10.1128/MCB.22.22.7744-7757.2002

Itoh, T., A. Toh-E, and Y. Matsui. 2004. Mmr1p is a mitochondrial factor for Myo2p-dependent inheritance of mitochondria in the budding yeast. *EMBO J.* 23:2520–2530. doi:10.1038/sj.emboj.7600271

Kemper, C., S.J. Habib, G. Engl, P. Heckmeyer, K.S. Dimmer, and D. Rapaport. 2008. Integration of tail-anchored proteins into the mitochondrial outer membrane does not require any known import components. *J. Cell Sci.* 121:1990–1998. doi:10.1242/jcs.024034

Kornmann, B., E. Currie, S.R. Collins, M. Schuldiner, J. Nunnari, J.S. Weissman, and P. Walter. 2009. An ER-mitochondria tethering complex revealed by a synthetic biology screen. *Science*. 325:477–481. doi:10.1126/science.1175088

Lillie, S.H., and S.S. Brown. 1994. Immunofluorescence localization of the unconventional myosin, Myo2p, and the putative kinesin-related protein, Smy1p, to the same regions of polarized growth in *Saccharomyces cerevisiae*. *J. Cell Biol.* 125:825–842. doi:10.1083/jcb.125.4.825

Matsui, Y. 2003. Polarized distribution of intracellular components by class V myosins in *Saccharomyces cerevisiae*. *Int. Rev. Cytol.* 229:1–42. doi:10.1016/S0074-7696(03)29001-X

Merz, S., M. Hammermeister, K. Altmann, M. Dürr, and B. Westermann. 2007. Molecular machinery of mitochondrial dynamics in yeast. *Biol. Chem.* 388:917–926. doi:10.1515/BC.2007.110

Mnaimneh, S., A.P. Davierwala, J. Haynes, J. Moffat, W.T. Peng, W. Zhang, X. Yang, J. Pootoolal, G. Chua, A. Lopez, et al. 2004. Exploration of essential gene functions via titratable promoter alleles. *Cell*. 118:31–44. doi:10.1016/j.cell.2004.06.013

Motley, A.M., G.P. Ward, and E.H. Hettema. 2008. Dnm1p-dependent peroxisome fission requires Caf4p, Mdv1p and Fis1p. *J. Cell Sci.* 121:1633–1640. doi:10.1242/jcs.026344

Pashkova, N., N.L. Catlett, J.L. Novak, and L.S. Weisman. 2005a. A point mutation in the cargo-binding domain of myosin V affects its interaction with multiple cargoes. *Eukaryot. Cell*. 4:787–798. doi:10.1128/EC.4.4.787-798.2005

Pashkova, N., N.L. Catlett, J.L. Novak, G. Wu, R. Lu, R.E. Cohen, and L.S. Weisman. 2005b. Myosin V attachment to cargo requires the tight association of two functional subdomains. *J. Cell Biol.* 168:359–364. doi:10.1083/jcb.200407146

Pashkova, N., Y. Jin, S. Ramaswamy, and L.S. Weisman. 2006. Structural basis for myosin V discrimination between distinct cargoes. *EMBO J.* 25:693–700. doi:10.1038/sj.emboj.7600965

Pathak, D., K.J. Sepp, and P.J. Hollenbeck. 2010. Evidence that myosin activity opposes microtubule-based axonal transport of mitochondria. *J. Neurosci.* 30:8984–8992. doi:10.1523/JNEUROSCI.1621-10.2010

Peraza-Reyes, L., D.G. Crider, and L.A. Pon. 2010. Mitochondrial manoeuvres: latest insights and hypotheses on mitochondrial partitioning during mitosis in *Saccharomyces cerevisiae*. *Bioessays*. 32:1040–1049. doi:10.1002/bies.201000083

Pon, L.A. 2008. Golgi inheritance: rab rides the coat-tails. *Curr. Biol.* 18:R743–R745. doi:10.1016/j.cub.2008.07.002

Prinz, W.A., L. Grzyb, M. Veenhuis, J.A. Kahana, P.A. Silver, and T.A. Rapoport. 2000. Mutants affecting the structure of the cortical endoplasmic reticulum in *Saccharomyces cerevisiae*. *J. Cell Biol.* 150:461–474. doi:10.1083/jcb.150.3.461

Pruyne, D., A. Legesse-Miller, L. Gao, Y. Dong, and A. Bretscher. 2004. Mechanisms of polarized growth and organelle segregation in yeast. *Annu. Rev. Cell Dev. Biol.* 20:559–591. doi:10.1146/annurev.cellbio.20.010403.103108

Quintero, O.A., M.M. DiVito, R.C. Adikes, M.B. Kortan, L.B. Case, A.J. Lier, N.S. Panaretos, S.Q. Slater, M. Rengarajan, M. Feliu, and R.E. Cheney. 2009. Human Myo19 is a novel myosin that associates with mitochondria. *Curr. Biol.* 19:2008–2013. doi:10.1016/j.cub.2009.10.026

Reck-Peterson, S.L., D.W. Provance Jr., M.S. Mooseker, and J.A. Mercer. 2000. Class V myosins. *Biochim. Biophys. Acta*. 1496:36–51. doi:10.1016/S0167-4889(00)00007-0

Reynolds, E.S. 1963. The use of lead citrate at high pH as an electron-opaque stain in electron microscopy. *J. Cell Biol.* 17:208–212. doi:10.1083/jcb.17.1.208

Rossanese, O.W., C.A. Reinke, B.J. Bevis, A.T. Hammond, I.B. Sears, J. O'Connor, and B.S. Glick. 2001. A role for actin, Cdc1p, and Myo2p in the inheritance of late Golgi elements in *Saccharomyces cerevisiae*. *J. Cell Biol.* 153:47–62. doi:10.1083/jcb.153.1.47

Schott, D., J. Ho, D. Pruyne, and A. Bretscher. 1999. The COOH-terminal domain of Myo2p, a yeast myosin V, has a direct role in secretory vesicle targeting. *J. Cell Biol.* 147:791–808. doi:10.1083/jcb.147.4.791

Schott, D.H., R.N. Collins, and A. Bretscher. 2002. Secretory vesicle transport velocity in living cells depends on the myosin-V lever arm length. *J. Cell Biol.* 156:35–39. doi:10.1083/jcb.200110086

Seabra, M.C., and E. Coudrier. 2004. Rab GTPases and myosin motors in organelle motility. *Traffic*. 5:393–399. doi:10.1111/j.1398-9219.2004.00190.x

Shaner, N.C., R.E. Campbell, P.A. Steinbach, B.N. Giepmans, A.E. Palmer, and R.Y. Tsien. 2004. Improved monomeric red, orange and yellow fluorescent proteins derived from *Discosoma* sp. red fluorescent protein. *Nat. Biotechnol.* 22:1567–1572. doi:10.1038/nbt1037

Shepard, K.A., A.P. Gerber, A. Jambhekar, P.A. Takizawa, P.O. Brown, D. Herschlag, J.L. DeRisi, and R.D. Vale. 2003. Widespread cytoplasmic mRNA transport in yeast: identification of 22 bud-localized transcripts using DNA microarray analysis. *Proc. Natl. Acad. Sci. USA*. 100:11429–11434. doi:10.1073/pnas.2033246100

Sherman, F. 1964. Mutants of yeast deficient in cytochrome c. *Genetics*. 49:39–48.

Sherman, F. 1991. Getting started with yeast. *Methods Enzymol.* 194:3–21. doi:10.1016/0076-6879(91)94004-V

Sikorski, R.S., and P. Hieter. 1989. A system of shuttle vectors and yeast host strains designed for efficient manipulation of DNA in *Saccharomyces cerevisiae*. *Genetics*. 122:19–27.

Smith, J.J., M. Marelli, R.H. Christmas, F.J. Vizeacoumar, D.J. Dilworth, T. Ideker, T. Galitski, K. Dimitrov, R.A. Rachubinski, and J.D. Aitchison. 2002. Transcriptome profiling to identify genes involved in peroxisome assembly and function. *J. Cell Biol.* 158:259–271. doi:10.1083/jcb.200204059

Sogo, L.F., and M.P. Yaffe. 1994. Regulation of mitochondrial morphology and inheritance by Mdm10p, a protein of the mitochondrial outer membrane. *J. Cell Biol.* 126:1361–1373. doi:10.1083/jcb.126.6.1361

Sparkes, I.A., N.A. Teanby, and C. Hawes. 2008. Truncated myosin XI tail fusions inhibit peroxisome, Golgi, and mitochondrial movement in tobacco leaf epidermal cells: a genetic tool for the next generation. *J. Exp. Bot.* 59:2499–2512. doi:10.1093/jxb/ern114

Stürmer, K., and O. Baumann. 1998. Immunolocalization of a putative unconventional myosin on the surface of motile mitochondria in locust photoreceptors. *Cell Tissue Res.* 292:219–227. doi:10.1007/s004410051053

Trybus, K.M. 2008. Myosin V from head to tail. *Cell. Mol. Life Sci.* 65:1378–1389. doi:10.1007/s00018-008-7507-6

Valiathan, R.R., and L.S. Weisman. 2008. Pushing for answers: is myosin V directly involved in moving mitochondria? *J. Cell Biol.* 181:15–18. doi:10.1083/jcb.200803064

Wang, Z., and T.C. Pesacreta. 2004. A subclass of myosin XI is associated with mitochondria, plastids, and the molecular chaperone subunit TCP-1alpha in maize. *Cell Motil. Cytoskeleton*. 57:218–232. doi:10.1002/cm.10168

Warren, G., and W. Wickner. 1996. Organelle inheritance. *Cell*. 84:395–400. doi:10.1016/S0092-8674(00)81284-2

Weisman, L.S. 2006. Organelles on the move: insights from yeast vacuole inheritance. *Nat. Rev. Mol. Cell Biol.* 7:243–252. doi:10.1038/nrm1892

Westermann, B., and W. Neupert. 2000. Mitochondria-targeted green fluorescent proteins: convenient tools for the study of organelle biogenesis in *Saccharomyces cerevisiae. Yeast*. 16:1421–1427. doi:10.1002/1097-0061(200011)16:15<1421::AID-YEA624>3.0.CO;2-U

Wiedemann, N., C. Meisinger, and N. Pfanner. 2009. Cell biology. Connecting organelles. *Science*. 325:403–404. doi:10.1126/science.1178016

Yaffe, M.P. 1999. The machinery of mitochondrial inheritance and behavior. *Science*. 283:1493–1497. doi:10.1126/science.283.5407.1493

Youngman, M.J., A.E. Hobbs, S.M. Burgess, M. Srinivasan, and R.E. Jensen. 2004. Mmm2p, a mitochondrial outer membrane protein required for yeast mitochondrial shape and maintenance of mtDNA nucleoids. *J. Cell Biol.* 164:677–688. doi:10.1083/jcb.200308012

Zheng, M., Q. Wang, Y. Teng, X. Wang, F. Wang, T. Chen, J. Samaj, J. Lin, and D.C. Logan. 2010. The speed of mitochondrial movement is regulated by the cytoskeleton and myosin in *Picea wilsonii* pollen tubes. *Planta*. 231:779–791. doi:10.1007/s00425-009-1086-0